A Benthic-optimised Marine Environment Classification (BOMEC) for New Zealand waters

J.R. Leathwick
A. Rowden
S. Nodder
R. Gorman
S. Bardsley
M. Pinkerton
S.J. Baird
M. Hadfield
K. Currie
A. Goh

NIWA
Private Bag 14901
Wellington 6241

New Zealand Aquatic Environment and Biodiversity Report No. 88
2012

Published by Ministry of Fisheries
Wellington
2012

ISSN 1176-9440

Leathwick, J.R.; Rowden, A.; Nodder, S.; Gorman, R.; Bardsley, S.; Pinkerton, M.;
Baird, S.J.; Hadfield, M.; Currie, K.; Goh, A. (2012).
A Benthic-optimised Marine Environment Classification (BOMEC) for New Zealand waters.
New Zealand Aquatic Environment and Biodiversity Report No. 88. 54p.

This series continues the
Marine Biodiversity Biosecurity Report series
which ceased with No. 7 in February 2005.

EXECUTIVE SUMMARY

Leathwick, J.R.; Rowden, A.; Nodder, S.; Gorman, R.; Bardsley, S.; Pinkerton, M.; Baird, S.J.; Hadfield, M.; Currie, K.; Goh, A. (2012). A benthic-optimised marine environment classification (BOMEC) for New Zealand waters.

***New Zealand Aquatic Environment and Biodiversity Report No. 88.* 54 p.**

Distributional data for eight taxonomic groups (asteroids, bryozoans, benthic foraminiferans, octocorals, polychaetes, matrix-forming scleractinian corals, sponges, and benthic fish) have been used to train an environmental classification for those parts of New Zealand's 200 n. mile Exclusive Economic Zone (EEZ) with depths of 3000 m or less. A variety of environmental variables were used as input to this process, including estimates of depth, temperature, salinity, sea surface temperature gradient, surface water productivity, suspended sediments, tidal currents, seafloor sediments, and seabed relief. These variables were transformed using results averaged across eight Generalised Dissimilarity Modelling analyses that indicate relationships between species turnover and environment for each species group. The matrix of transformed variables was then classified using k-medoids clustering to identify an initial set of 300 groups of cells based on their environmental similarities, with relationships between these groups then described using agglomerative hierarchical clustering. Groups at a fifteen group level of classification appropriate for use at a whole-of-EEZ scale are described. The classification can also be used at other levels of detail, for example when higher levels of classification detail are required to discriminate variation within study areas of more limited extent. Although not formally tested in this analysis, we expect the analytical process used here to increase the biological discrimination of the environmental classification. That is, the resulting environmental groups are more likely to have similar biological characteristics than when the input environmental variables are selected, weighted, and perhaps transformed using qualitative methods. As a consequence, they are more likely to be reliable when used as “habitat classes” for the management of biological values than groups defined using alternative approaches.

1. INTRODUCTION

Environmental classifications are a potentially powerful tool for summarising broadscale spatial patterns in ecosystem character, particularly when biological data are limited in availability (Pressey et al. 2000, Leathwick et al. 2003). This relies on consistency of relationships between biological patterns and some set of environmental factors and is a particularly practical approach when spatial variation in those environmental factors can be relatively easily measured or modelled. A marine classification using this approach, the Marine Environment Classification (MEC) has already been developed for New Zealand's 200 n. mile Exclusive Economic Zone (EEZ) (Snelder et al. 2004, Snelder et al. 2006). The MEC is generic, i.e., it classifies patterns for both the pelagic and benthic elements of the marine ecosystem. A more specifically tailored classification has been defined to discriminate variation in demersal fish community composition (Leathwick et al. 2006a).

One feature of the MEC approach is the ability to improve the biological discrimination of a classification both by choosing appropriate defining variables (the environmental variables used as input to the classification process), and then applying appropriate weightings and transformations to them (Snelder et al. 2007). Giving greater weight to the dominant drivers of biological patterns increases their influence on classification outcomes, and transformation can linearise the relationship between species turnover and individual drivers, making them more effective in summarising broad-scale biological patterns when classified using standard multivariate techniques.

In the generic MEC defined by Snelder et al. (2004, 2007), a relatively simple approach was used to select, weight, and transform environmental variables with which to define the classification. This used the Mantel test to measure correlations between matrices containing estimates of biological and environmental differences between pairs of sites drawn from various biological datasets. Environmental variables identified as dominant were given increased influence by including them more than once, and transforms were applied using a relatively restricted set of parametric options.

In a more recent classification defined for New Zealand's rivers and streams, Leathwick et al. (2011) demonstrated the use of a more sophisticated approach based around Generalised Dissimilarity Modelling (GDM – Ferrier et al. 2007). This applies a more refined implementation of matrix regression that specifically accommodates both 1) the curvilinear relationship between ecological distance and compositional dissimilarity between sites, and 2) variation in the rate of compositional turnover both between and along environmental gradients. Rather than using parametric transforms of the environmental variables, GDM uses flexible I-splines that are constrained to be positively monotonic, this capturing the manner in which biological differences between sites generally increase with increasing separation along environmental gradients. As in conventional spline-based regression, the amplitudes of the fitted functions control the magnitude of the contributions associated with each environmental gradient fitted in the final model.

In conceptual terms, GDM offers some particular advantages when dealing with data that are sparse, or describe the distributions of very large numbers of species (Ferrier et al. 2007). When the available compositional data are of high quality one can model directly the biological patterns, either by classifying the sample sites into groups and interpolating these spatially on the basis of environment, or alternatively by interpolating the distributions of individual species, and then classifying the resulting predictions (e.g., Leathwick et al. 2006b). However, when the available biological data are sparse, relative to compositional turnover, the data will be insufficient to adequately define all the community groups occurring in a study site. In this setting, GDM constructs a broader and more encompassing model of the general relationship between species turnover (β-diversity) and the different environmental drivers of these patterns. This model can then be used in a variety of ways, including (i) as a continuous model of environmental space in the which transformations applied to the environmental axes maximize the capture of variation in species composition, or (ii) as a basis for classification, in which the transformed environmental space is divided up into groups or categories, also maximising the ability to summarise biological patterns.

In the freshwater classification defined by Leathwick et al. (2011), separate GDM analyses were performed using distributional data sets for freshwater fish and macro-invertebrates. The fitted functions for each variable were averaged across these analyses, and these averaged functions were then applied to environmental data for all rivers and stream segments throughout New Zealand. The final transformations expressed by these functions captured both variation in weighting to reflect the differing importance of environmental variables, and transformation to account for different rates of species turnover along each environmental gradient. After classification of the transformed matrix, the biological discrimination of the groups generated was compared with that of groups defined in two previous classifications, and the results indicated a generally superior ability to summarise biological patterns.

Here we apply the same GDM-based approach across New Zealand's EEZ to define a classification specifically designed to assess and manage the impacts of bottom trawling on benthic organisms: benthic-optimised marine environment classification (BOMEC). Environmental data are drawn from the previous MEC, supplemented by additional data layers developed since to address particular gaps (Pinkerton & Richardson 2005, Pinkerton et al. 2005) (see Appendices 1–5). Biological data used to guide the classification process were drawn from a variety of sources and describe the distributions of eight different taxonomic groups: benthic fish species and seven benthic invertebrate groups. Thus, this work and that presented by Baird & Wood (2012) address the following objective of Ministry of Fisheries-contracted project BEN2006/01: to integrate information on the distribution, frequency, and magnitude of fishing disturbance with habitat characteristics throughout the EEZ, using information stored in national databases, expert opinion, and the MEC.

2. METHODS

2.1 Species data

Species records were assembled separately for each of eight taxonomic groups; asteroids, bryozoans, benthic foraminiferans, octocorals, polychaetes, matrix-forming scleractinian corals, sponges, and benthic fish (Table 1). These taxonomic groups are some of the relatively few groups of invertebrates for which available data represent species level identifications that are consistent across the entire New Zealand EEZ (i.e., original identifications by the same taxonomist or identifications that have been checked and modified where appropriate by a single taxonomist). These taxonomic groups are also useful for the purpose of the classification because they allow for the representation of species with a range of trophic (functional) modes of life (polychaetes); that are numerical or biomass dominants in particular substrates or locations (foraminiferans, polychaetes, asteroids, sponges); that would be expected to be particularly vulnerable to disturbance by bottom fishing (bryozoans, octocorals, matrix-forming scleractinian corals, sponges); and would be expected *a priori* to occur throughout the entire three-dimensional space of the EEZ (all groups with the exception of corals, sponges and foraminiferans whose lowest depth limit will be constrained the availability of particular chemical compounds). Data for invertebrate species groups were extracted from distributional databases held by NIWA, with additional records for foraminiferans provided by B. Hayward (Geomarine Research). Some of these invertebrate data are available from the South Western Pacific Regional Ocean Biogeographic Information System (OBIS) portal (http://obis.niwa.co.nz).

Data describing the distributions of 38 benthic fish species were taken from a version of the Research Trawl Database (FishComm database) that was extensively groomed by NIWA staff. Selected species were predominantly flatfish (flounder and rays) and predominantly bottom-dwelling species such as eels, gurnard, and stargazers. Records for the taxonomic groups were identified to the level of individual species, apart from the octocorals which were recorded only to the level of family and the polychaetes which were variable (but mostly at species level). All sets of records were separately edited by (i) converting any records of abundance to presence/absence (0/1), (ii) removing species with fewer than five occurrences, and (iii) removing sites with no species once rare species had been deleted.

Table 1: Biological data sets used in the analyses.

Taxonomic group	No. samples	No. taxa	Taxa/sample	Taxonomic resolution	Source
Asteroids	2 348	97	1.7	Species	NIWA data/OBIS
Bryozoans	552	272	11.3	Species	NIWA data/OBIS
Benthic fish	15 825	38	3.9	Species	FishComm database
Foraminiferans	241	397	34.7	Species	NIWA data supplemented with records from B. Hayward/OBIS
Octocorals	596	17	1.4	Family	NIWA data
Polychaetes	1 476	185	3.6	Variable	NIWA data/OBIS
Matrix-forming scleractinian corals	318	6	1.1	Species	NIWA data
Sponges	88	49	4.6	Species	NIWA data

There was strong variation in numbers of sites, geographic coverage, and depth coverage in the final edited datasets (see Table 1). Numbers of samples ranged from 88 for sponges to nearly 16 000 for fish. There was also marked variation between the datasets, both in total numbers of species and average numbers of species per sample. The foraminiferan dataset contained the greatest number of species, both overall (397) and per sample (mean = 34.7); the bryozoan and polychaete datasets also had high total numbers of species, but lower numbers of species per sample. The two coral datasets had the lowest numbers of taxa, both in total and average per sample. Geographic coverage was reasonable in shallower waters for most datasets, but several had major gaps in coverage in deeper waters, including the datasets for fish and foraminiferans, which also completely lacked samples in the northern part of New Zealand's EEZ around the Kermadec Islands. Some datasets had relatively poor coverage of samples on the large area of the Campbell Plateau (polychaetes, octocorals, matrix-forming scleractinian corals, sponges) (Figure 1). Most datasets had reasonable depth coverage down to about 1500 m (Figure 2), but with proportionally fewer samples below that — exceptions were the polychaete and sponge datasets, both of which had a low proportion of samples below about 500 m.

2.2 Environmental predictors

Environmental predictors (Table 2), chosen for their functional relevance, were derived for all sample sites by overlay onto gridded data layers at a resolution of 1 km, stored in a GIS. Depth was one of the main predictors used, but in conceptual terms it is generally recognised as functioning as an indirect surrogate for a range of more proximate drivers of biological pattern, including several that have an influence upon the occurrence of benthic fauna (e.g., light, temperature, pressure, oxygen) (e.g., Snelder et al. 2006). Although some of these other factors can be predicted from statistical and/or process-based models, many are so strongly correlated with depth that their individual contributions cannot be discriminated with statistically based modelling techniques such as those used for our main analyses. For this reason, we restricted the range of depth-correlated variables, including only estimates of the mean annual salinity and temperature at the seafloor, which were derived by combining coarser resolution (quarter of a degree) descriptions of temperature and salinity from the World Ocean Atlas (Boyer et al. 2005) with a New Zealand-wide, 1 km resolution bathymetry layer (Pinkerton et al. 2005), while also applying some local smoothing.

Because the high correlation between depth and temperature still had considerable potential to confound subsequent model fitting, we normalised temperature estimates with respect to depth. That is, we described the average relationship between depth and temperature for all grid cells by fitting a Generalised Linear Model that related temperature to depth using a non-linear (natural spline) function. Residuals from this model indicate the departure in degrees at each grid cell from the overall trend.

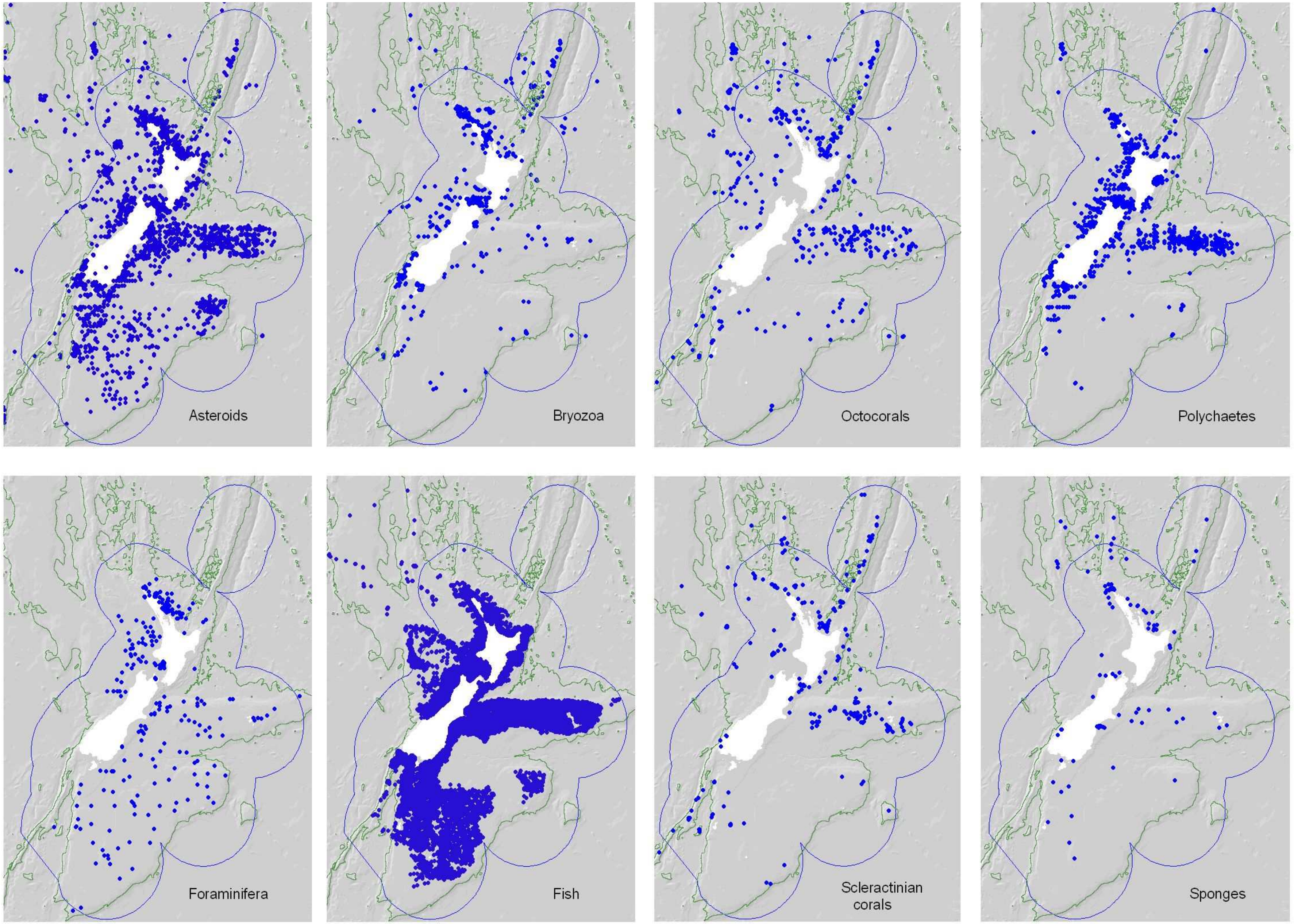

Figure 1: Geographic distributions of samples for the eight biological group datasets.

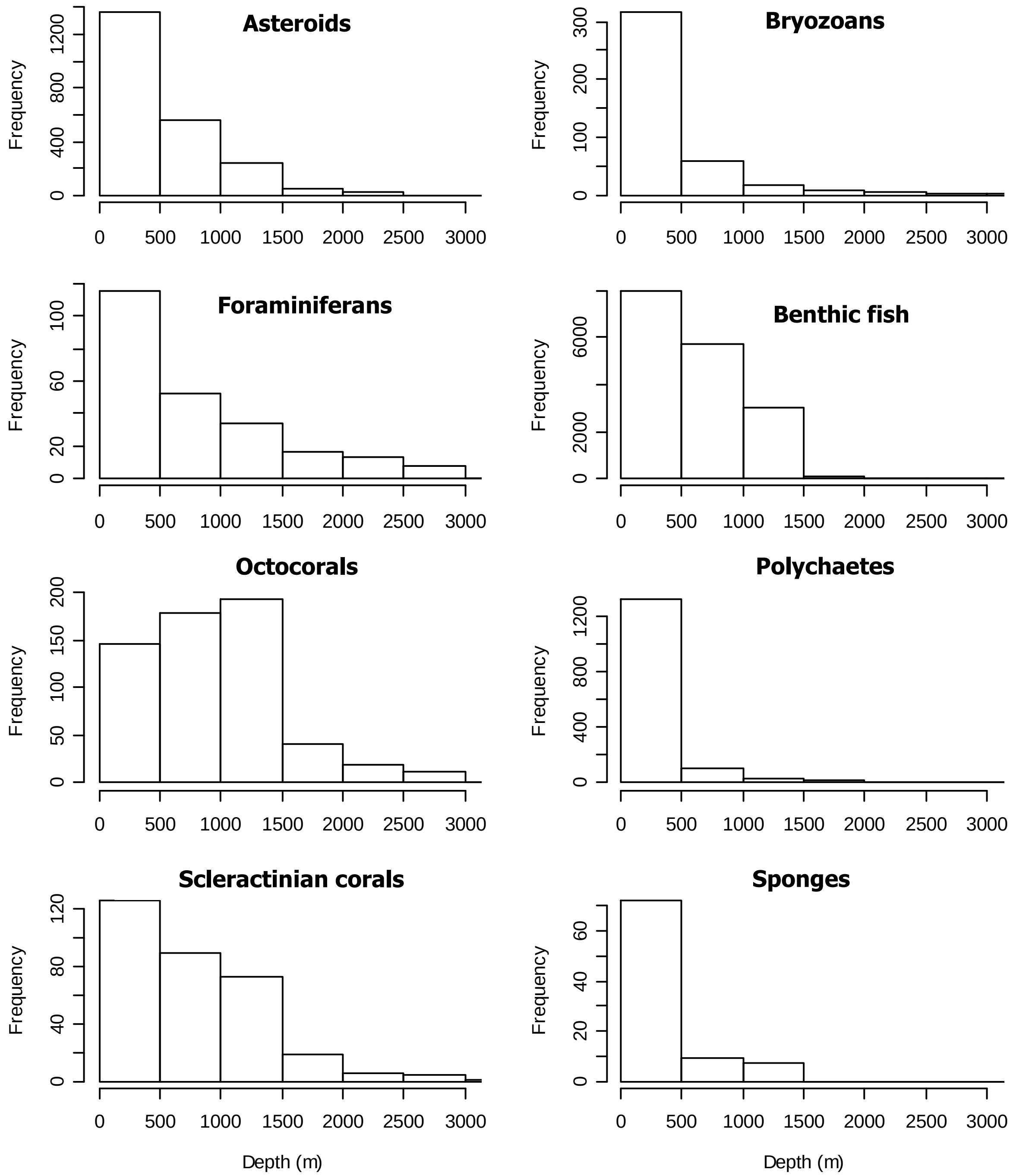

Figure 2: Depth distributions of biological datasets used to train the GDM classification. Note differing scales on the vertical axes.

Estimates of the spatial gradient in annual sea surface temperature, which indicates zones of intense mixing of water bodies, were derived from remote sensing data (Snelder et al. 2004). These zones or fronts of oceanic water masses have been found to define the boundaries of particular benthic assemblages, because the physico-chemical characteristics of a water mass influence benthic assemblage composition (e.g., Watling & Gerkin 2005).

Estimates of surface water primary productivity were derived from the Vertically Generalized Production Model (VGPM) of Behrenfeld & Falkowski (1997), using estimates of chlorophyll concentration derived from Sea-WiFS data for the period from 1997–2006 (M. Pinkerton, NIWA, pers. comm., see Appendix 4). Surface water primary production is an important source of detrital food for benthic organisms, which is thought to be one of the main environmental drivers of benthic faunal patterns in the deeper waters of the ocean (Levin et al. 2001).

Substrate type (typically described by the predominant sediment size class or category) is often evoked as the main factor influencing the distribution of benthic assemblages. However, it is a number of sedimentary and hydrodynamic variables associated with determining substrate type that indirectly and directly control the occurrence of benthic organisms, and which are more likely to have predictive capability (Snelgrove & Butman 1994).

Estimates of depth-averaged tidal currents were derived from tidal models (Snelder et al. 2004), and descriptions of the predominant sediment size were derived from published charts (NZOI and NIWA sediment chart series), interpolated and interpreted using expert opinion to overcome inconsistencies in the recording of sediment classes and categories across the EEZ (see Appendix 1). No attempt was made to include data describing the origins of different sediments, e.g., biogenic versus terrigenous sediments.

Estimates of average orbital wave velocities at the seafloor were derived from modelled estimates of wave conditions in the New Zealand region over a 20–year period (Gorman & Laing 2000), and this information was combined with the sediment size information to estimate the average proportion of time during which seafloor velocities exceeded those required to resuspend seabed sediments (see Appendix 2).

Bottom currents derived from tides and/or waves can control the distribution of benthic organisms that either cannot withstand high current conditions (e.g., fragile taxa with delicate feeding apparatus) or require such currents to transport sufficient food that they can recover from the water (e.g., suspension/filter feeding taxa). Bottom current dynamics can therefore be responsible for assemblage composition patterns between and within taxonomic groups (e.g., benthic foraminiferan assemblages, Debenay et al. 2005). Sediment resuspension events influence the flux of nutrients and organic matter at the sediment-water interface (e.g., Tengburg et al. 2003), which in turn can control the composition of benthic assemblages (e.g., Tahey et al. 1994).

The coarse resolution of the bathymetry layer meant that it was not sensible to calculate seabed slope; instead we calculated for each cell the standard deviation of depths in a surrounding 3 x 3 km neighbourhood, a measure of seabed relief. Seabed relief will influence the occurrence of benthic fauna, either directly through the provision of habitat of different characteristics or indirectly where relief is significantly elevated for topographically induced flow to control assemblage composition (e.g., corals on ridges and seamount peaks (Genin et al. 1986)).

Table 2: Environmental predictors used in the analyses.

Predictor	Derivation	Mean [range]
Depth (m)	From bathymetric maps	1289 [0–3000]
Temperature (ºC)	World Ocean Atlas, normalised to depth	0.026 [-8.1–9.900]
Salinity (psu)	World Ocean Atlas	34.6 [34.2–35.6]
SST gradient (ºC km^{-1})	SeaWiFS imagery	0.0013 [0.000–0.1057]
Productivity (mgC m^{-2} d^{-1})	Modelled	452 [170–2404]
Tidal current (m s^{-1})	Modelled	0.15 [0.00–3.16]
Sediment size (mm)	Sediment charts	0.35 [0.00–10.00]
Orbital velocity (dm s^{-1})	Wave model	9.6 [0.0–2445.0]
Sediment resuspension	Wave model and sediment data	-9.16 [-10.00–0.41]
Suspended particulate matter (arbitrary units)	Remote sensed	0.162 [0.040–68.880]
Dissolved organic matter (arbitrary units)	Remote sensed	0.035 [0.000–5.880]
Seabed relief	Standard deviation of depths in a 3 by 3 km neighbourhood	16.33 [0.00–656.40]

Estimates of suspended particulate and dissolved organic matter were both derived from satellite imagery using a case-2 algorithm (Pinkerton & Richardson 2005). Riverine inputs of sediment can affect the distribution of benthic organisms (generally at local scales, but also at relatively large spatial scales where river inputs are high) (e.g., Aller & Stupakoff 1996) and levels of suspended particulate matter and dissolved organic matter in coastal environments act as useful proxies for the physical and chemical influence of river discharges.

2.3 GDM analyses

All analyses were performed using Generalised Dissimilarity Modelling (GDM – Ferrier et al. 2007), a technique that models variation in species turnover between sites as a function of environment. This uses a modified form of matrix regression to model the relationship between biological and environmental distances between pair-wise combinations of sites. It accommodates the generally asymptotic nature of the relationship between biological and environmental distances using an appropriate link function and fits positively monotonic splines to describe rates of species turnover in relation to a set of environmental predictors.

A single GDM analysis was performed for each of the six smaller datasets, and the fitted functions were extracted using a small set of environmental data containing 200 evenly spaced points along the ranges of each of the predictor variables. Because GDM is relatively demanding of memory, the two larger datasets (asteroids and benthic fish) were repeatedly sub-sampled, subsets of 1400 sites being randomly selected and analysed, with the fitted functions stored and then averaged to derive a final set of transforms. A record was also kept of the deviance explained by each of the repeated models for both these datasets, and these were averaged on completion to give a single estimate of model explanation.

2.4 Defining a classification

Results from the GDM analyses were then combined to create a data matrix for classification in which the raw environmental values were transformed using the fitted functions from the GDM analyses, averaged across the eight taxonomic groups.

The starting point for this part of the analysis was a matrix of untransformed values for each of the 12 predictors for each of 244 000 grid cells, each of 1 km^2 and covering all of New Zealand's EEZ down to a depth of 3000 m, i.e., the approximate lower depth limit beyond which minimal biological samples were available. Transforms from each of the GDM analyses for the eight taxonomic groups were applied separately to the raw input data, and values were then averaged for each cell and predictor across the resulting eight transformed matrices.

Because of the very large size of the final transformed matrix, it was classified in two stages, the first using a relatively memory-efficient, non-hierarchical method to define a reduced set of initial groups, with relationships between these then defined using a more demanding, hierarchical clustering technique. Initial clustering into 200 groups was performed using k-medoids clustering, a more robust variant of k-means clustering, contained in the 'cluster' library in R. The manhattan metric was used as a distance measure, preserving the transformed matrix values from the GDM analyses; i.e., it applies no range-standardisation or other transformation to the input data.

Average (transformed) values from these groups were then exported and hierarchically clustered in pattern analysis software (PATN – Belbin 1991), again using the manhattan metric. Flexible agglomerative clustering (flexible Unweighted Pair Group Method with Arithmetic Mean (UPGMA – Belbin 1991)) was used for this analysis with a value for β of -0.1 which applies slight space dilation, discouraging the formation of small outlier groups and generally giving more interpretable clusters (Belbin et al. 1992). Results from these analyses were imported into a GIS and visual inspection of both the geographic distributions of groups and similarities between them were used to select an appropriate level of classification detail for initial description. Higher levels of classification detail could be used for applications requiring greater detail.

3. RESULTS

3.1 GDM analyses

There was marked variation in the explanatory power of the GDM analyses between the different taxonomic groups, mostly reflecting the adequacy of sampling methods for the sampled taxa (Table 3). For example, the deviance explained exceeded 40% for the fish and foraminiferan datasets, both of which have large sample areas relative to the sizes and densities of the sampled individuals, resulting in the samples carrying a large amount of information about the species composition at each site. The lowest amount of deviance was explained for octocorals; these were identified only to a family level and had only a small number of taxa both per sample and overall. The sponge dataset showed a higher level of deviance explained than the other small datasets, suggesting strong patterns of sorting in this group. Most of the species groups included 10 or 11 of the 12 environmental predictors available, but only eight and nine predictors were used in the matrix-forming scleractinian coral and sponge datasets respectively.

Trends in species turnover for the different groups are indicated by the functions fitted by the GDM analyses, typical graphs of which are presented for one group (asteroids) in Figure 3. Functions fitted for all eight taxonomic groups are presented in Appendix 6. In the example shown, the fitted functions indicate that maximum species turnover for asteroids occurs in relation to depth, i.e., the function showing the largest range of values. Local changes in the slopes of the functions are also informative, indicating variation in rates of species turnover along the range of each environmental predictor. For example in Figure 3, turnover rates are relatively uniform along the entire length of both the sediment size and seafloor temperature gradients; by contrast, changes in species turnover in relation to depth are more rapid in shallow (less than 250 m) than deeper waters, as indicated by the steeper slope at the left-hand end of this curve. Similarly, species turnover in relation to suspended particulate matter is initially rapid, but stabilises once values for this predictor exceed 15.

Summaries of the maximum values of the fitted functions for the different taxonomic groups and environmental predictors (Table 4) indicate that species turnover is generally strongest in relation to depth; it was the single most important predictor for five of the eight groups and had the highest average overall. Exceptions to this pattern were as follows: in the octocorals, the seafloor temperature anomaly variable was most important predictor; in the bryozoans, salinity had the strongest effect; and in the sponges, seafloor sediment resuspension was the strongest predictor. Note that in the latter dataset, sediment resuspension was highly correlated with depth, so some inter-substitution could be occurring between predictors. Temperature was also important for other taxonomic groups, ranking second in importance for asteroids and polychaetes, and third for bryozoans and sponges. Salinity was the second most important predictor for matrix-forming scleractinian corals. The least frequently fitted predictor was seafloor sediment resuspension, which was included in models for only four of the eight taxonomic groups.

Table 3: Summary statistics for GDM analyses of eight taxonomic groups of benthic species.

Species group	Repeats	Deviance explained (%)	No. predictors
Asteroids	100	8.8	10.2 (8–11)
Bryozoans	1	16.0	11
Benthic fish	100	44.0	10.7 (8–12)
Foraminiferans	1	49.7	10
Octocorals	1	2.6	11
Polychaetes	1	12.8	11
Matrix-forming scleractinian corals	1	15.1	8
Sponges	1	26.4	9

Comparison of the maximum function values averaged across the predictors fitted for each taxonomic group (bottom row of Table 4) indicates that total species turnover is strongest in the asteroid and polychaete datasets and weakest in the foraminiferan dataset. This is consistent with the characteristics of the datasets as recorded in Table 1, where the total number of species recorded in the asteroid and polychaete datasets is approximately fifty times their respective averages for number of species per sample. By contrast, the total number of species recorded in the foraminiferan dataset, which shows lowest levels of species turnover, is only about 10 times the average number of species per sample.

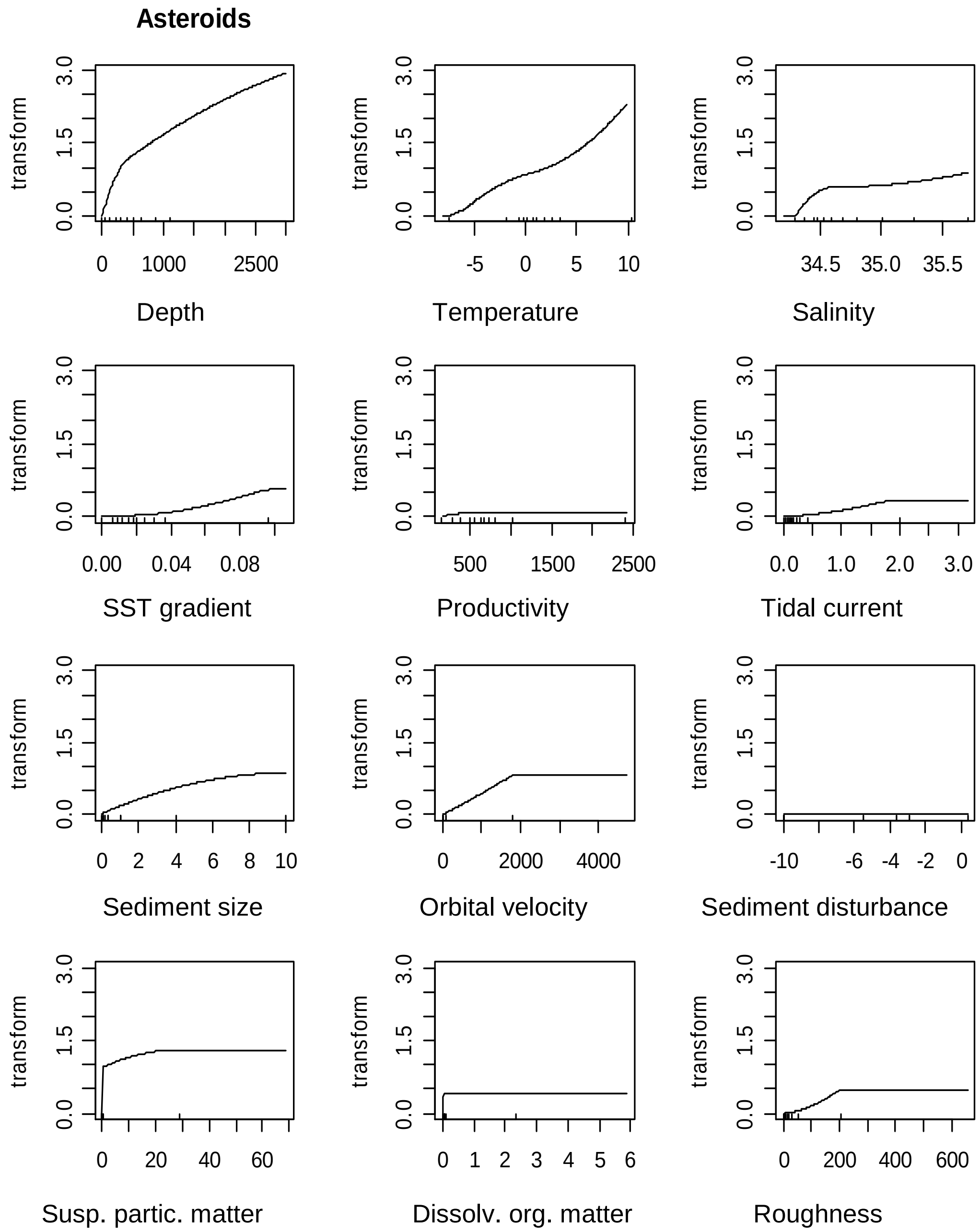

Figure 3: Functions fitted by GDM analyses of the relationship between species turnover and environment for the asteroid dataset, averaged across 100 models.

Table 4: Maximum values of functions fitted environmental predictors in GDM analyses of species turnover for eight taxonomic groups of benthic species. The predictor value with the greatest range for each dataset is shown in bold type. See Table 2 for predictor measures.

	Asteroids	Bryozoans	Benthic fish	Foraminiferans	Octocorals	Polychaetes	Matrix-forming scleratinians	Sponges	All
Depth	**2.94**	0.98	**5.11**	**0.63**	0.14	**2.4**	**2.32**	0.82	1.92
Temperature	**2.28**	**1.01**	**0.18**	**0.22**	**1.2**	**1.84**	**0.46**	**0.96**	**1.02**
Salinity	0.89	**1.98**	0.24	0.02	0.24	0.17	1.62	0.01	0.64
SST Gradient	0.55	0.77	0.09	0.24	0.81	0.45	0.18	1.36	0.56
Suspended particulate matter	1.3	0.43	0.29	0.08	0.53	1.21	0.21	–	0.51
Tidal current	0.34	1.17	0.07	0.22	0.11	1.36	–	0.45	0.47
Orbital velocity	0.81	0.31	0.91	–	–	0.52	0.29	0.79	0.45
Dissolved organic matter	0.43	0.96	0.36	–	0.49	–	1.02	0.28	0.44
Productivity	0.08	0.9	0.21	0.21	0.58	1.49	–	–	0.43
Seabed relief	0.5	0.34	0.11	0.27	0.12	1.17	0.35	–	0.36
Sediment size	0.87	0.58	0.12	0.24	0.3	0.4	–	0.04	0.32
Sediment resuspension	–	–	0.14	0.21	0.11	0.24	–	**1.6**	0.29
Average	0.92	0.79	0.65	0.2	0.39	0.94	0.54	0.52	

Averaging the fitted functions across the eight taxonomic groups (Figure 4) produces a final set of transforms in which depth has the dominant effect, with high initial species turnover moderating gradually with increasing depth. The final averaged functions for temperature and salinity, the next most important predictors, are relatively linear, but stepped functions are fitted for several of the remaining minor predictors; i.e., rapid initial change occurs over a relatively narrow range of values, but is muted thereafter (e.g., the fitted function for suspended particulate matter or dissolved organic matter).

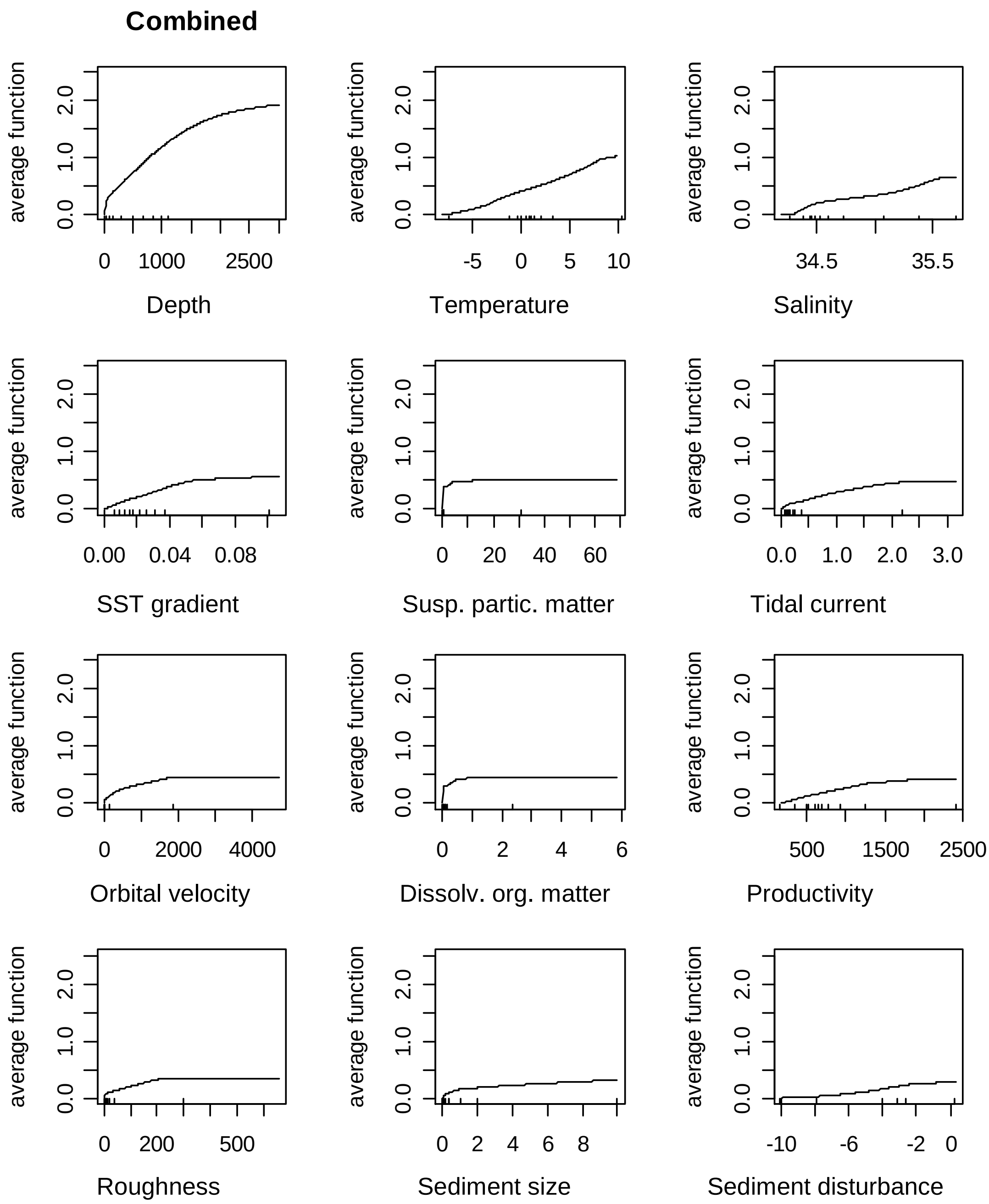

Figure 4: Functions fitted by GDM analyses of the relationship between species turnover and environment, averaged across the eight taxonomic groups. Predictors are sorted in decreasing order according to their maximum values.

3.2 Classification

Fifteen groups have been recognised as providing an appropriate level of detail for a broad-scale classification of New Zealand's EEZ to a depth of 3000 m (Figure 5, Table 5). These groups are strongly separated in relation to depth, comprising three inshore groups (A, B, and D), three shelf groups (C, E, and F), and nine groups in deeper waters of the continental slope and troughs (G–O). Sorting is also apparent in relation to other environmental factors, particularly in shallow waters, but this becomes progressively muted with increasing depth, reflecting the much greater homogeneity of conditions there.

The first four groups (A–D) vary most strongly with respect to depth, temperature, salinity, sediment size, and seafloor sediment resuspension. Group A is the most northern, occurring mostly around the coast of the North Island, including in the Hauraki Gulf and Hawke Bay; it also occurs in shallow, inshore waters along the west coast of the South Island and in Golden Bay. It has the highest temperature and salinity of all groups and also has high levels of suspended particulate matter and dissolved organic matter; both productivity and sediment resuspension of the seafloor are high. Group B is more southern in distribution, occurring predominantly along the western and northern coasts of the South Island and in slightly deeper waters than the previous group. It has lower temperature and salinity, but slightly higher productivity and finer sediments than the previous group. Group C occurs in more offshore locations than the previous two groups, and is extensive on the continental shelf around the North Island and along the South Island's west coast. Temperature and salinity are moderately high, sediments are relatively fine, and seafloor sediment resuspension is lower than in the two previous groups because of the greater depth. Group D occurs at shallow depths along the eastern and southern coasts of the South Island; both water temperature and salinity are lower than in the preceding groups, but sediments are coarser.

Groups E–H occur largely in the more offshore waters of the continental shelf and upper continental slope, mostly from about Cook Strait south. Group E occurs along the east coast of the South Island south to the Stewart-Snares shelf, on the Mernoo Bank, the Veryan Bank, and around the Chatham Islands; whereas Group F occurs on the shelves surrounding New Zealand's more southern sub-Antarctic islands (Auckland, Campbell, Bounty) and on the Pukaki Rise. The latter has the colder temperatures and lower salinity; both have strong tidal currents and coarse sediments. Group E has strong sea surface temperature gradients along the well defined boundary between sub-tropical and sub-Antarctic waters that occurs along the Southland coast. Groups G and H occur in deeper waters along the upper continental slope; Group G is the more restricted in occurrence and occurs in areas of steep topography with very strong tidal currents, mostly around the eastern entrance to Cook Strait, and along the south-western coast of the South Island; it also occurs locally near East Cape. Group H occurs both along the crest of the Chatham Rise and at similar depths around both main islands (including the shallower depths of the Challenger Plateau). It has moderately high temperatures and salinity, reflecting the influence of sub-tropical waters.

Groups I–K occur at lower slope depths, mostly in northern and central waters, but vary markedly in geographic extent. Group I is largely restricted to sites along the southern flanks of the Chatham Rise and the eastern slope of the Stewart-Snares shelf and has lower temperature and salinity values being south of the Subtropical Front. Group J is much more extensive and occurs along both the north and south of the Chatham Rise, on the Challenger Plateau, and around the North Island; it also occurs off the Fiordland coast at the northern end of the Solander Trough. Temperature, salinity, and productivity are slightly higher than in the previous group. Group K is the most restricted in extent, found in very steep sites off North Cape; it has warm temperatures and strong tidal currents.

Groups L and M occupy similar depths to the previous three groups, but with a more southerly bias in distribution, and this is reflected in their generally lower temperatures and salinity. Their productivity is also lower than in the previous three groups. Both occur on the generally gently sloping Campbell and Bounty Plateaux, with Group M occurring in deeper waters than Group L.

The last two groups, N and O, occupy the deepest waters with Group N averaging nearly 1400 m on the upper parts of the troughs and Group O averaging nearly 2400 m in depth in the lower parts of the troughs. Both occur over a wide latitudinal range, have low sea surface temperature gradients and tidal currents, and fine sediments.

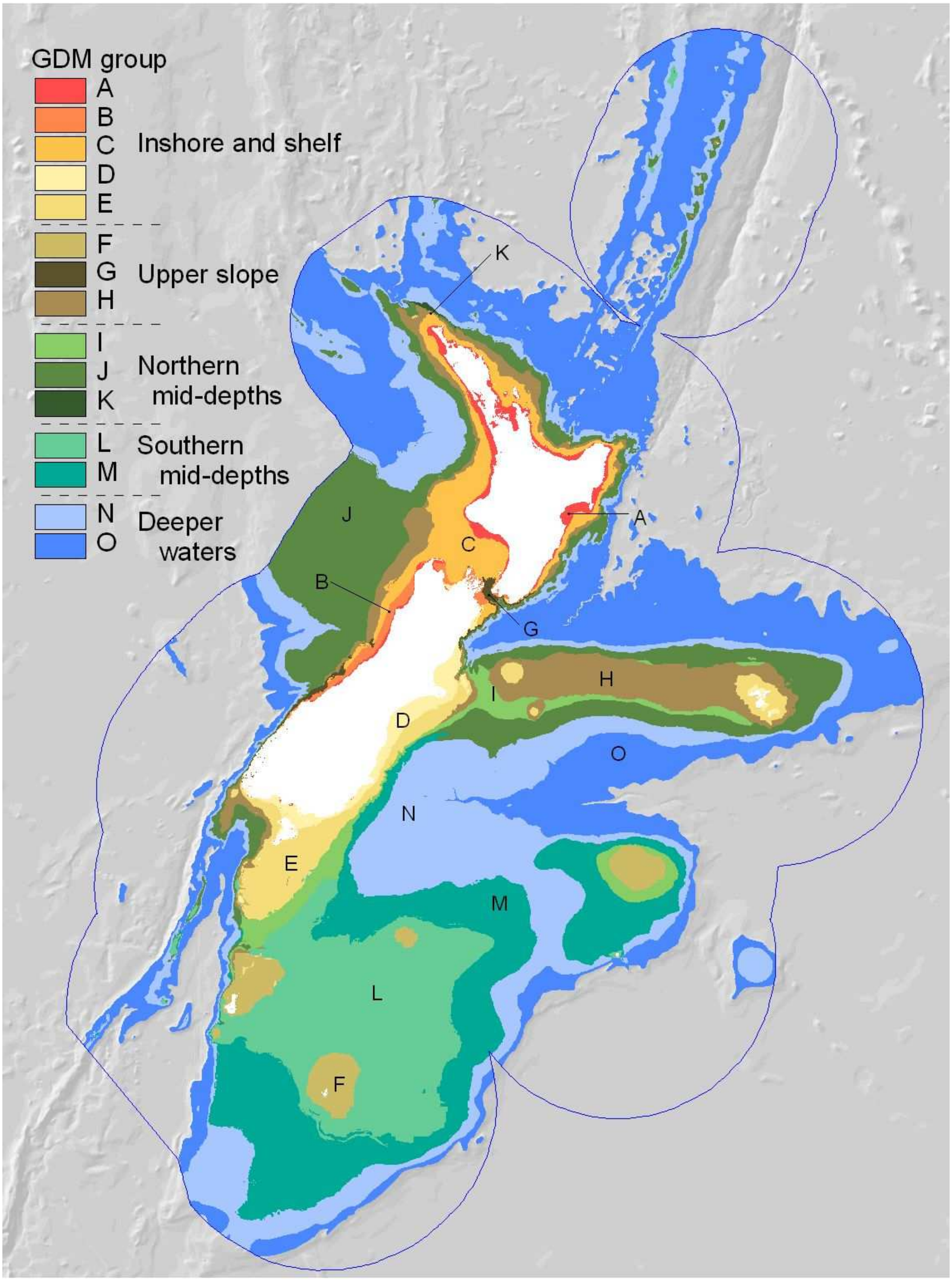

Figure 5: Geographic distribution of groups defined by multivariate classification of environmental data transformed using results from GDM analyses of relationships between environment and species turnover averaged across eight taxonomic groups of benthic species.

Table 5: Geographic extent (calculated using the Albers equal area projection) and environmental averages of 15 groups defined by a classification in which variable weighting and transformation was guided by results averaged GDM analyses of eight taxonomic groups of benthic species. A bold horizontal line indicates separation at a two-group level of classification, and two further lines indicate divisions to give a four group level of classification. Parameter measures are given in Table 2.

Group	Extent (km^2)	Depth	Temperature anomaly	Salinity	SST Gradient	Productivity	Tidal current	Sediment size	Orbital velocity	Sediment resuspension	Suspended pm.	Dissolved org. matt.	Relief
A	27 557	25.6	2.59	35.35	0.015	1 333.6	0.20	1.66	317.5	-2.7	1.63	0.22	4.0
B	12 420	63.9	0.74	35.05	0.027	1 490.7	0.26	0.43	123.7	-2.7	0.83	0.20	6.7
C	89 710	104.7	2.06	35.27	0.018	950.7	0.28	0.56	36.9	-3.3	0.23	0.07	4.1
D	27 268	38.6	-2.07	34.65	0.020	888.7	0.30	1.97	269.1	-2.9	0.83	0.15	4.1
E	60 990	136.3	-1.26	34.65	0.030	500.1	0.50	2.46	50.8	-3.6	0.18	0.06	6.3
F	38 608	178.1	-2.96	34.43	0.007	299.4	0.45	2.88	50.1	-4.2	0.15	0.04	5.2
G	6342	230.5	1.02	34.93	0.026	1 060.6	0.51	0.88	20.2	-6.1	0.34	0.10	45.1
H	138 550	337.0	1.27	34.75	0.026	674.5	0.26	0.60	0.4	-7.8	0.17	0.06	10.8
I	52 224	559.8	-0.47	34.41	0.033	452.0	0.21	0.42	0.0	-9.9	0.17	0.05	11.4
J	311 361	834.4	0.95	34.51	0.015	574.3	0.15	0.22	0.0	-10.0	0.15	0.04	15.9
K	1 290	1 018.3	1.20	34.91	0.051	691.8	0.46	0.61	0.0	-9.1	0.14	0.04	92.5
L	198 577	531.0	-0.38	34.42	0.007	230.5	0.17	0.43	0.0	-9.2	0.12	0.02	3.5
M	233 825	883.7	-0.64	34.35	0.009	234.2	0.12	0.08	0.0	-10.0	0.12	0.02	5.9
N	493 034	1 397.5	0.00	34.53	0.011	379.4	0.10	0.13	0.0	-10.0	0.13	0.03	18.1
O	935 315	2 343.7	0.00	34.67	0.011	469.9	0.08	0.13	0.0	-10.0	0.13	0.03	27.7

4. DISCUSSION AND CONCLUSIONS

The analysis presented here demonstrates the broad feasibility of the use of GDM to allow the integration of analyses across a number of biological datasets, this having particular value in that it allows each individual dataset to contribute equally to the final classification, regardless of sample size. The use of spline functions in GDM also allows a very flexible approach to the selection, weighting, and transformation of the candidate environmental variables. While we have not formally tested the biological discrimination of the resulting classification, results from other analyses (Leathwick et al. 2011) indicate that this should be higher than for classifications defined using variables selected and weighted using more subjective approaches.

The BOMEC is of potentially more relevance for evaluating and managing human activities at the seafloor than the MEC, and here we briefly assess the similarity or otherwise of the two classifications. Figure 6 reveals that the 15 class level BOMEC has parallels and differences when compared with the generic 20 class level MEC (when restricted to the EEZ and 3000 m the latter is represented by 18 classes). For example, both the MEC and BOMEC identify nearshore and shelf classes (e.g., 64, 60 and A, C). The BOMEC classes show more discrimination of the nearshore waters around the South Island. Distinct classes are identified in the Cook Strait region for both the MEC and BOMEC (58 and G, respectively); however these classes are also found off North Cape (MEC) and the slope south west of the South Island (BOMEC). The boundaries of upper slope areas represented by the MEC class 63 (which includes the Challenger Plateau and the Chatham Rise) are broadly similar to class J of the BOMEC, with the notable exception of the further subdivision of the Chatham Rise area into three shallower classes for the latter classification (E, H, I: only one of which is similar to a MEC class). The Campbell Plateau is largely represented by class 178 in the MEC, whilst for the BOMEC a similar area comprises at least five classes. Overall, a north-south distribution pattern of classes is more evident in the MEC whereas the BOMEC classes are distributed more strongly with reference to water depth. The BOMEC, even at the 15 class level, provides a higher degree of spatial partitioning in deeper waters than the MEC and identifies at least two classes (G and K) which do not have corollaries in the MEC.

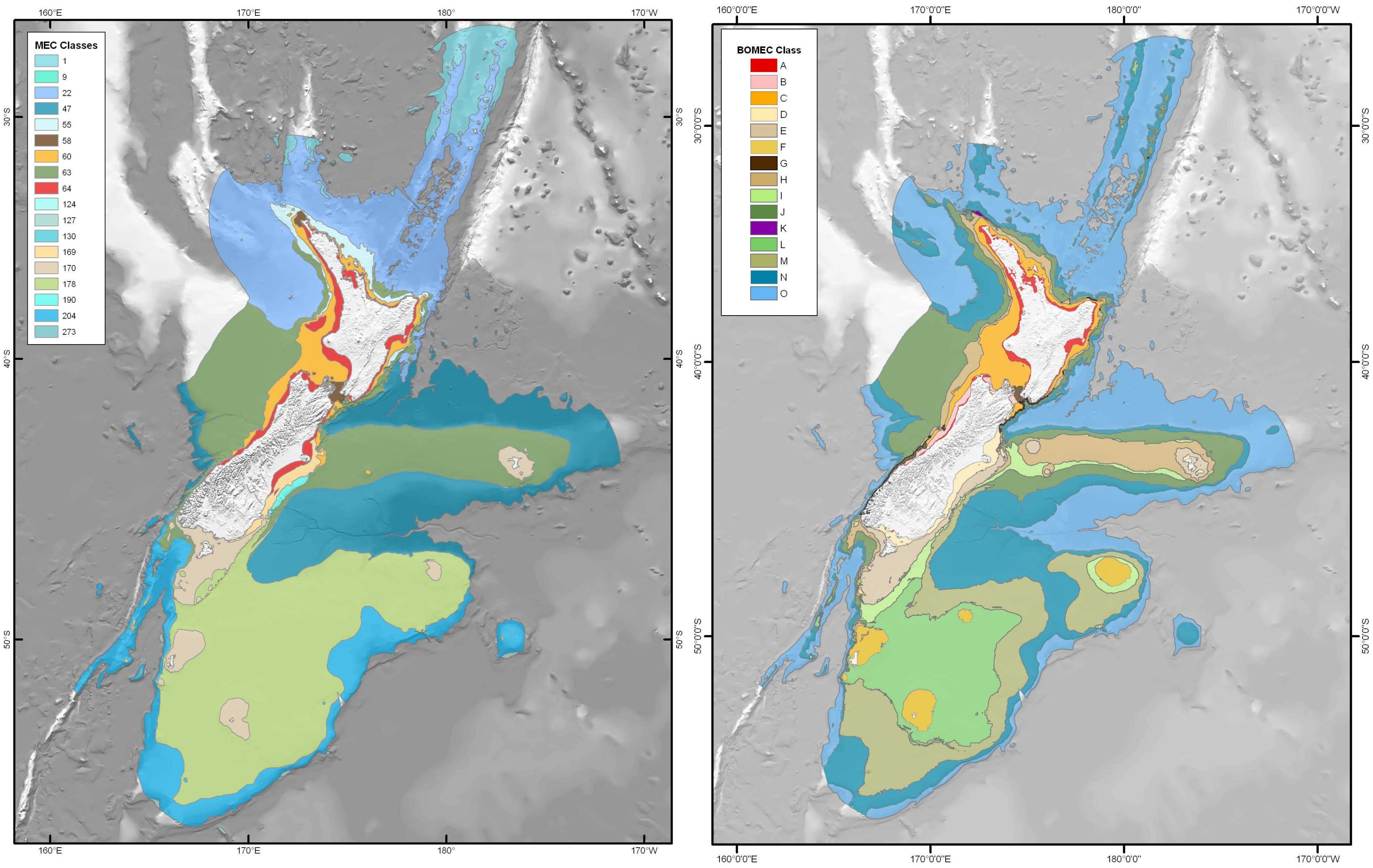

Figure 6: Geographic distribution of classes defined by the MEC by Snelder et al. (2006) (left) and by BOMEC (right). The MEC classes have been restricted to those in depths down to 3000 m (18 classes), and BOMEC classes have been recoloured to allow comparison between the two distributions.

We note that further improvement of the BOMEC is possible in the distributional data used for this analysis. Benefits would come from improving the taxonomic resolution in the polychaete and octocoral datasets; the addition of new datasets describing the distributions of ophiuroids, molluscs, and decapods would provide a more complete taxonomic coverage of the major benthic species groups occurring in New Zealand's marine environments.

Further improvement would also be possible in the environmental data used in the analysis, both with respect to the selection of variables used, and their spatial resolution. For example, building higher resolution bathymetry datasets for inshore waters would allow increased resolution for depth and temperature, the dominant drivers in this analysis, and this would give the biggest gains in terms of improving this classification. The development of a higher resolution, regional-scale ocean climatology would also deliver improvements in the temperature and salinity layers compared with the broad scale World Oceans Atlas data used here, particularly if it used more comprehensive regional data sets coupled with an improved bathymetry layer. Flow on improvements from an improved bathymetry layer would also potentially occur in our tidal current, orbital velocity, sediment resuspension, and seabed relief layers.

Another recent development is a nutrient-surface temperature relationship that provides better spatial coverage for nutrients than the World Data Atlas for the New Zealand region (Sherlock et al. 2007). Several of the other layers are based on remote sensed data with a resolution of 4 km, mostly from the SeaWiFS satellite. Replacement products, based on data from the higher resolution (1 km) Modis satellite are being developed and should be available in the next 12–18 months. New products that model the flux of organic matter to the seabed are also now becoming available (e.g., Lutz et al. 2007). Further work on the refinement of the sediment grain size and compositional data, and thus reconciliation between the different chart types, would provide a more consistent sediment distribution across the EEZ and increase the rigour of derived parameters such as sediment disturbance that are fundamental to understanding the benthic environment. In particular, only about 50% of the Coastal Sediment Chart series have been completed around the NZ coastline, the more regional charts are over 25 years old, and new multi-beam data are providing additional data on substrate distributions.

Finally, further improvement is probably also likely in our use of GDM once we are able to fully explore the sensitivity of results to the various analytical choices made in this analysis, and to explore alternative ways of accommodating large data sets and analyses carried out across several groups of species. We have since used GDM in an analysis of freshwater ecosystem patterns, and results in that work are similar to those achieved here, which gives us confidence that the approach used here is generally robust. We are also carrying out additional work to explore how best to optimise the use of GDM, and this is likely to improve our understanding of how to achieve the best results with what is a complex tool — both to understand and use.

Building these improvements in both biological and environmental data would allow the production of an operational classification with a range of levels of classification detail (rather than the static 15 layer version used here) as implemented for example in the current MEC and FWENZ products. Production of higher resolution versions for inshore waters at a resolution of say 200 m would also be feasible, and could prove to be a powerful tool to support a range of management activities, including for example, the implementation of a robust set of Marine Protected Areas.

5. ACKNOWLEDGEMENTS

Both Simon Ferrier (CSIRO, Canberra) and Jane Elith (University of Melbourne) provided helpful comments on the use of GDM with multiple groups of species, and Glenn Manion (NSW Environment and Conservation, Armidale) helped resolve some initial analytical difficulties. This work was completed under Objective 5 of BEN200601 for the Ministry of Fisheries.

6. REFERENCES

Aller, J.Y.; Stupakoff, I. (1996). The distribution and seasonal characteristics of benthic communities on the Amazon shelf as indicators of physical processes. *Continental Shelf Research 16*: 717–751.

Baird, S.J.; Wood, B.A. (2012). Extent of coverage of 15 environmental classes within the New Zealand EEZ by commercial trawling with seafloor contact. *New Zealand Aquatic Environment and Biodiversity Report No.89.* 43 p.

Behrenfeld, M.J.; Falkowski, P. (1997). A consumer's guide to phytoplankton primary productivity models. *Limnology & Oceanography 42*: 1479–1491.

Belbin, L. (1991). PATN Technical Reference Manual. CSIRO Division of Wildlife & Ecology, Canberra.

Belbin, L.; Faith, D.P.; Milligan, G.W. (1992). A comparison of two approaches to beta-flexible clustering. *Multivariate Behavioural Research 27*: 417–433.

Boyer, T.; Levitus, S.; Garcia, H.; Locarnini, R.; Stephens, C.; Antonov, J. (2005). Objective analyses of annual, seasonal, and monthly temperature and salinity for the world on a 1/4degree Grid. *International Journal of Climatology 25*: 931–945.

Debenay, J.P.; Millet, B.; Angelidis, M.O. (2005). Relationships between foraminiferal assemblages and hydrodynamics in the Gulf of Kalloni, Greece. *Journal of Foraminiferal Research 35*: 327–343.

Ferrier, S.; Manion, G.; Elith, J.; Richardson, K. (2007). Using generalised dissimilarity modelling to analyse and predict patterns of beta-diversity in regional biodiversity assessment. *Diversity and Distributions 13*: 252–264.

Genin, A.; Dayton, P.K.; Lonsdale, P.F.; Spiess, F.N. (1986). Corals on seamount peaks provide evidence of current acceleration over deep-sea topography. *Nature 322*: 59–61.

Gorman, R.M.; Laing, A.K. (2000). A long-term wave hindcast for the New Zealand coast. Paper presented at the 6th international workshop on wave hindcasting and forecasting, Monterey, California, November 2000.

Leathwick, J.; Dey, K.; Julian, K. (2006a). Development of an environmental classification optimised for demersal fish. NIWA Client Report: HAM2006-063. 20p. Available online at http://www.doc.govt.nz/upload/documents/conservation/marine-and-coastal/marine-protected-areas/MCU1.pdf

Leathwick, J.R., Francis, M., Julian, K. (2006b). Development of a demersal fish community classification for New Zealand's Exclusive Economic Zone. NIWA Client Report: HAM2006-062. 38p. Available online at: http://www.doc.govt.nz/upload/documents/conservation/marine-and-coastal/marine-protected-areas/MCU2.pdf

Leathwick, J.R.; Overton, J.M.; McLeod, M. (2003). An environmental domain analysis of New Zealand, and its application to biodiversity conservation. *Conservation Biology 17*: 1612–1623.

Leathwick, J.R.; Snelder, T.; Chadderton, W.L.; Elith, J.; Julian, K.; Ferrier, S. (2011). Use of generalised dissimilarity modelling to improve the biological discrimination of river and stream classifications. *Freshwater Biology 56(1)*: 21–38.

Levin, L.A.; Etter, R.J.; Rex, M.A.; Gooday, A.J.; Smith, C.R.; Pineda, J.; Stuart, C.T.; Hessler, R.R.; Pawson, D. (2001). Environmental influences on regional deep-sea species diversity. *Annual Review of Ecology and Systematics 32*: 51–93.

Lutz, M.J.; Caldeira, K.; Dunbar, R.B.; Behrenfeld, M.J. (2007). Seasonal rhythms of net primary production and particulate organic carbon flux describe biological pump efficiency in the global ocean. *Journal of Geophysical Research 112*. C10011, DOI:10.1029/2006JC003706. 26 p.

Pinkerton, M.; Hadfield, M.; Hunter, K.; Macaskill, B. (2005). Three additional layers for Marine Environment Classification: (1) Sea bed temperature; (2) Calcium compensation depth; (3) Sea-bed light levels. NIWA Client Report WLG2005–50. 40 p. Available at: http://www.doc.govt.nz/upload/documents/conservation/marine-and-coastal/marine-protected-areas/MCU6.pdf.

Pinkerton, M.H.; Richardson, K.R. (2005). Case 2 Climatology of New Zealand: Final report. NIWA Client Report WLG2005–49. 16 p. Available at: http://www.doc.govt.nz/upload/documents/conservation/marine-and-coastal/marine-protected-areas/MCU5.pdf

Pressey, R.L.; Hager, T.C.; Ryan, K.M.; Schwarz, J.; Wall, S.; Ferrier, S.; Creaser, P.M. (2000). Using abiotic data for conservation assessments over extensive regions: quantitative methods applied across New South Wales, Australia. *Biological Conservation 96*: 55–82.

Sherlock, V.; Pickmere, S.; Currie, K.; Hadfield, M.; Nodder, S.; Boyd, P.W. (2007). Predictive accuracy of temperature-nitrate relationships for the oceanic mixed layer of the New Zealand region. *Journal of Geophysical Research 112*, C06010, DOI:10.1029/2006JC003562.

Snelder, T.H., Dey, K.L., Leathwick, J.R. (2007). A procedure for making optimal selection of input variables for multivariate environmental classifications. *Conservation Biology 21*: 365–375.

Snelder, T.H.; Leathwick, J.R.; Dey, K.L.; Rowden, A.A.; Weatherhead, M.A.; Fenwick, G.D.; Francis, M.P.; Gorman, R.M.; Grieve, J.M.; Hadfield, M.G.; Hewitt, J.E.; Richardson, K.M.; Uddstrom, M.J.; Zeldis, J.R. (2006). Development of an ecological marine classification in the New Zealand region. *Environmental Management 39*: 12–29.

Snelder, T.; Leathwick, J.; Image, K.; Weatherhead, M.; Wild, M. (2004). The New Zealand Marine Environment Classification. NIWA Client Report CHC2004–071. 86 p.

Snelgrove, P.V.R.; Butman, C.A. (1994). Animal sediment relationships revisted – cause versus effect. *Oceanography and Marine Biology: An Annual Review 32*: 111–177.

Tahey, T.M.; Duineveld, G.G.A.; Berguis, E.M.; Helder, E.M. (1994). Relation between sediment-water fluxes of oxygen and silicate and faunal abundance at continental-shelf, slope and deep-water stations in the northwest Mediterranean. *Marine Ecology Progress Series 104*: 119–130.

Tengberg, A.; Almroth, E.; Hall, P. (2003). Resuspension and its effects on organic carbon recycling and nutrient exchange in coastal sediments: in situ measurements using new experimental technology. *Journal of Experimental Marine Biology and Ecology 285*: 119–142.

Watling, L.; Gerken, S. (2005). The Cumacea of the Faroe Islands region: water mass relationships and North Atlantic biogeography. *BIOFAR Proceedings 2005*: 137–149.

APPENDIX 1: SEDIMENT DATA

Prepared by Scott Nodder (marine geologist), Andrew Goh (sediment chart digitisation), Simon Bardsley (GIS).

Background

Sediment information is required as part of MFish contract BEN2006-01 to enable sediment disturbance by wave activity and sea-floor habitat diversity throughout New Zealand's Exclusive Economic Zone (EEZ) to be evaluated. The overall aim is to translate the sediment distribution data into a GIS framework and then incorporate these data into the NIWA Wave Model (e.g., WAM, Gorman et al. 2003a, b) to model potential wave disturbance and the Marine Environment Classification (e.g., Snelder et al. 2006) to relate marine physical parameters to benthic invertebrate and sediment distributions.

Sediment chart data

Sediment charts available for the project were published by the New Zealand Oceanographic Institute (NZOI), one of NIWA's parent organisations, over the period 1965 to 1992. These charts, and their published dates, were:

(1) New Zealand Regional Sediments, 1: 6 000 000 (Mitchell et al. 1989)
(2) Oceanic Series Sediment charts, 1: 1 000 000 scale: Three Kings (McDougall 1979), Cook (McDougall 1975) and Bounty (McDougall 1982).
(3) Coastal Series Sediment charts, 1:200 000 scale: Foveaux (Cullen & Gibb 1965), Mahia (Pantin & Gibb 1968), Turnagain (Lewis & Gibb 1970), Poor Knights (Eade 1974), Bay of Plenty (Doyle et al. 1979), Banks (Herzer 1979), Hauraki (Carter & Eade 1980), Cook Strait (Lewis & Mitchell 1980), Ellesmere (Herzer 1981), Raglan (Doyle & Arron 1982), Mokau (Arron & Doyle 1983), Oamaru (Arron 1986), Pegasus (Carter & Herzer 1986), Tasman (Mitchell 1987) and Patea (Nodder et al. 1992).

These charts depict the sediment distributions around New Zealand and the wider SW Pacific Ocean and eastern Tasman Sea using grain-size and compositional information collected from physical sea-floor samples by NZOI and other agencies, including the Royal Navy Hydrographic Office. Typically, distributions of different sediment types were interpreted and interpolated using geological knowledge and bathymetric data from complementary charts also produced by NZOI/NIWA. Only the NZ Regional Sediments chart covers the entire EEZ, but it does not have especially high spatial resolution, especially on the shelf. The three Oceanic Series charts cover a large part of the EEZ except off South West Fiordland, and the Coastal Series charts only cover approximately 50% of the New Zealand coastline. None of the chart series provide any accurate information on sediment distributions immediately adjacent to the coast, especially with regard to hard or rocky substrates. Clearly, there are also issues with sampling density over each of chart scales, such that variations in the sampling density, even from chart to chart within a series, will affect the amount of interpolation required to derive "sensible" sediment type boundaries. Finally, not all of the sediment samples were physically analysed to determine grain-size distributions with information also taken from the notations provided on British Admiralty and New Zealand Hydrographic charts and from visual observations of small samples. All of these factors impact on the reliability of the sediment distributions as portrayed on the charts.

Figure 1.1 shows the chart coverage used in the study. Each of the chart types listed above used different sediment classification schemes, as shown in Figures 1.2–1.5 and summarised in Table 1.1. This situation presents some difficulties in generating a coherent sediment distribution data-set across New Zealand's EEZ. For example, the NZ Regional Sediments 1: 6 000 000 chart (Mitchell et al. 1989) uses a simplified scheme whereby sediments are sub-divided on the basis of mineralogical composition and/or origin (e.g., Terrigenous, Biogenic, Deep Ocean Clays) with Dominant and Sub-dominant depicted, and the Terrigenous and Biogenic components further sub-divided on the basis of grain-size and/or composition. The Oceanic Series and the early renditions of the Coastal Series sediment charts (specifically, Foveaux, Turnagain, and Mahia) used a combination of grain-size and compositional information with Dominant (nominally more than 50% since this is not stated explicitly on the charts themselves) and Sub-dominant or Subsidiary types (more than 20%) specified. In contrast, most of the

Coastal Series charts from 1974 onwards adopted a ternary grain-size-based classification scheme, modified from Folk (1965), as well as delineated sediments that contained greater than or less than 50% calcium carbonate ($CaCO_3$) in composition. Furthermore, within the Coastal Series, some of the charts subdivided the mud fraction (less than 63 micron, µm) into silts (63–4 µm) and clays (less than 4 µm), whereas others only show "muddy" sediments.

To rationalise these sediment classification differences across the various chart types and their eras of publication, we have had to adopt a scheme that minimises the impact of these differences on the sediment distribution data required for the project. However, without going back to the original raw grain-size and compositional data and/or re-analysing the physical samples themselves, it is difficult to determine the validity of this rationalising scheme. Thus, there are still irreconcilable differences in sediment type across chart boundaries, such as within the Coastal Series depending on the date of chart publication and thus whether different classification schemes were used, and across boundaries between the NZ Regional Sediments, Oceanic and Coastal Series charts.

The sediment charts also depict locations of Consolidated Rock and note Specific Sedimentary Particles (Oceanic Sediment and pre-1974 Coastal Sediment charts) or Specific Grains (post-1974 Coastal Sediment charts). This information has not been incorporated into the present digitised dataset.

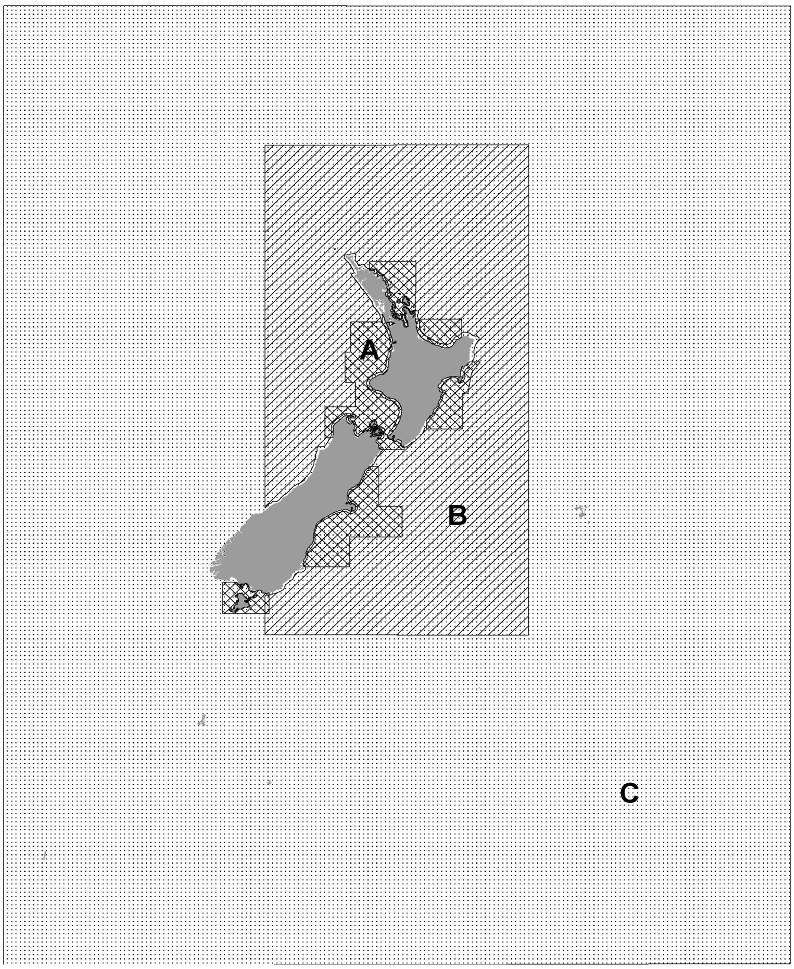

Figure 1.1: Summary figure showing the chart coverage used in the study. A is the Area of the published Coastal Sediment chart series, B the area of published Oceanic Sediment charts and C the extent of the NZ Regional Sediment Chart (Mitchell et al. 1989).

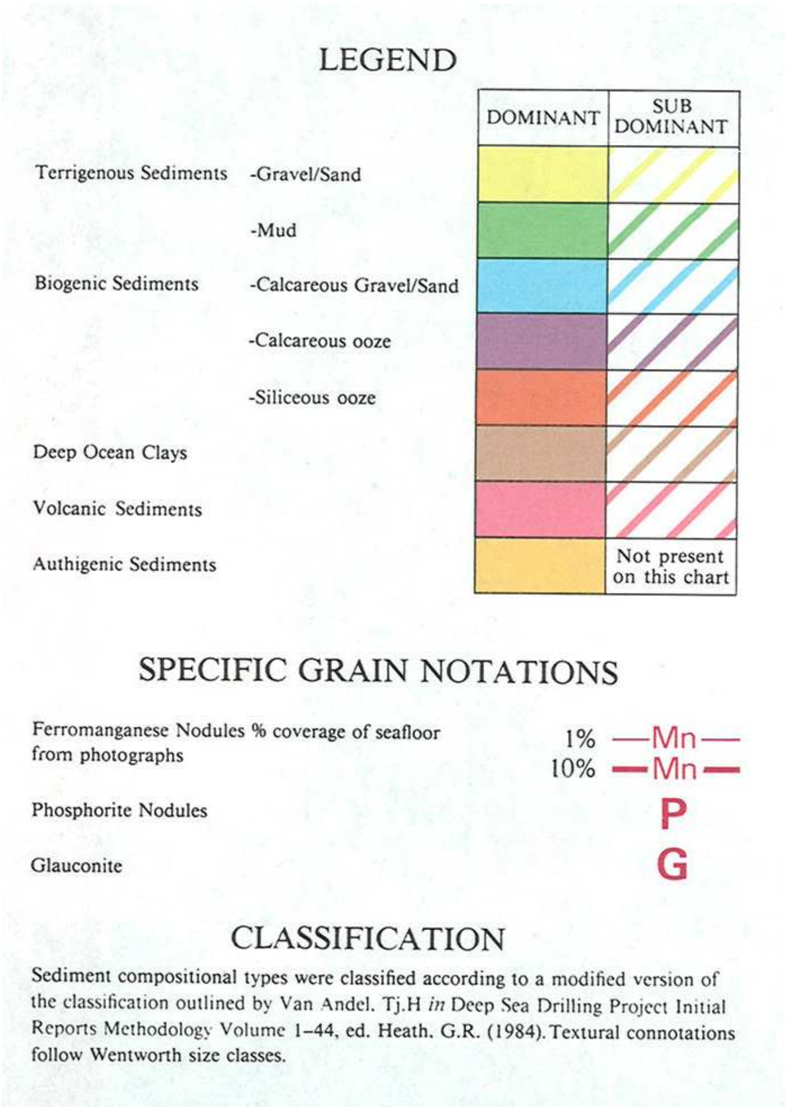

Figure 1.2: Sediment classification scheme used on NZ Regional Sediments chart (1:6 000 000, Mitchell et al. 1989).

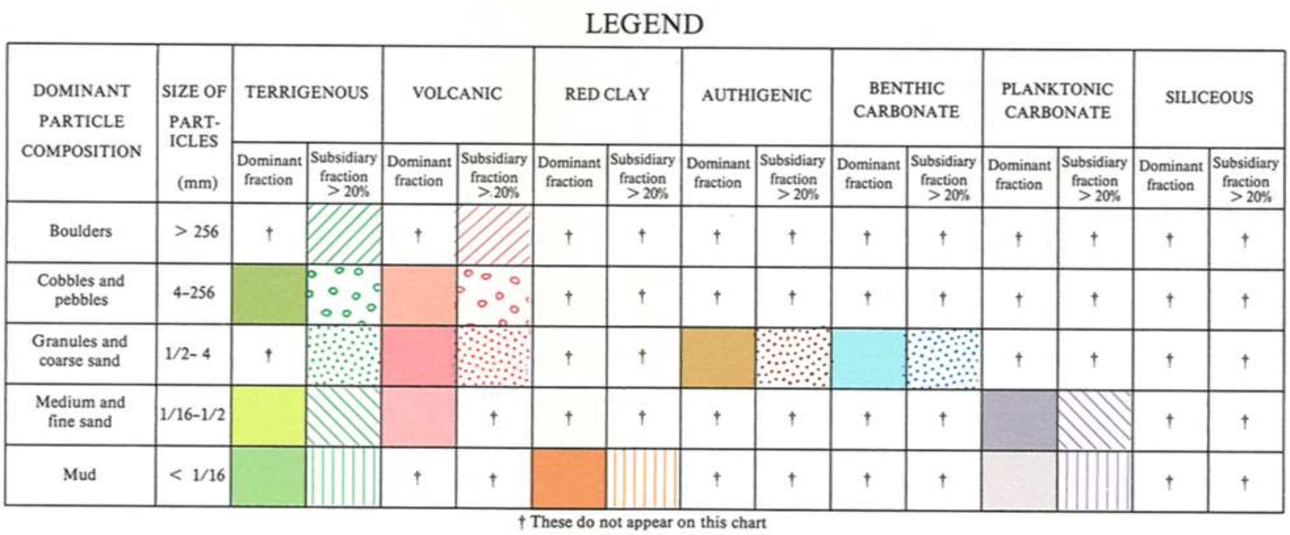

Figure 1.3: Sediment classification scheme used on Oceanic Sediment charts (1:1 000 000, McDougall 1975, 1979, & 1982).

COLOUR LEGEND

Dominant particle composition	Rock and mineral detritus			Organic carbonate remains (dead molluscan shell, bryozoa and coral skeletons, barnacle plates etc.)			Foraminiferal sediment		
	Dominant fraction	Subsidiary fraction > 20%	Size of particles (mm)	Dominant fraction	Subsidiary fraction > 20%	Size of particles (mm)	Dominant fraction	Subsidiary fraction > 20%	Size of particles (mm)
Boulders	†	†	> 256						
Cobbles and pebbles			4 – 256			> 4			
Granules and coarse sand			1/2 – 4			1/2 – 4	†	†	> 1/2
Medium and fine sand			1/16 – 1/2			1/16 – 1/2			1/16 – 1/2
Mud			< 1/16				†	†	< 1/16

† These do not appear on this chart

(a)

SEDIMENT CLASSIFICATION

Classification modified from Folk, R.L., 1965 : Petrology of Sedimentary Rocks, Hemphills Texas, 159pp.

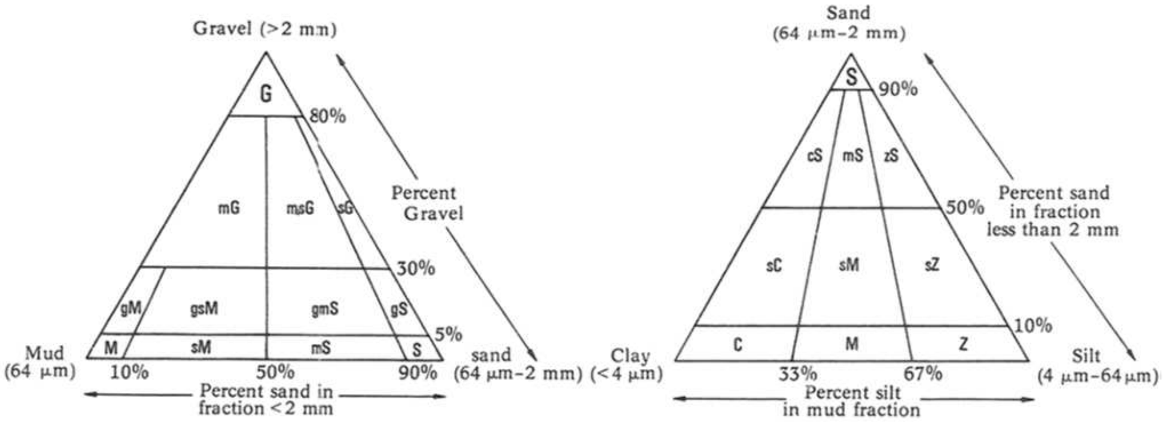

(b)

Note: M may be replaced by C or Z
m may be replaced by c or z

COLOUR LEGEND

	<50% Calcium Carbonate in gravel fraction		>50% Calcium Carbonate in gravel fraction	
G		gravel		calc-gravel
g		gravelly		calc-gravelly
	<50% Calcium Carbonate in sand fraction		>50% Calcium Carbonate in sand fraction	
S		sand		calc-sand
s		sandy		calc-sandy
	<50% Calcium Carbonate in mud fraction		>50% Calcium Carbonate in mud fraction	
Z		silt	†	calc-silt
z		silty	†	calc-silty
M		mud		calc-mud
m		muddy	†	calc-muddy
C	†	clay	†	calc-clay
c	†	clayey	†	calc-clayey

(c)

† Not present on this chart

Figure 1.4: Sediment classification schemes used on Coastal Sediment charts (1:200 000) (a) Categories used on Foveaux (1965), Mahia (1967), and Turnagain charts (1970); (b) Adapted Folk ternary classification scheme used on Coastal Sediment charts post-1970; (c) Categories used on Coastal Sediment charts post-1970 based on the Folk classification in (b).

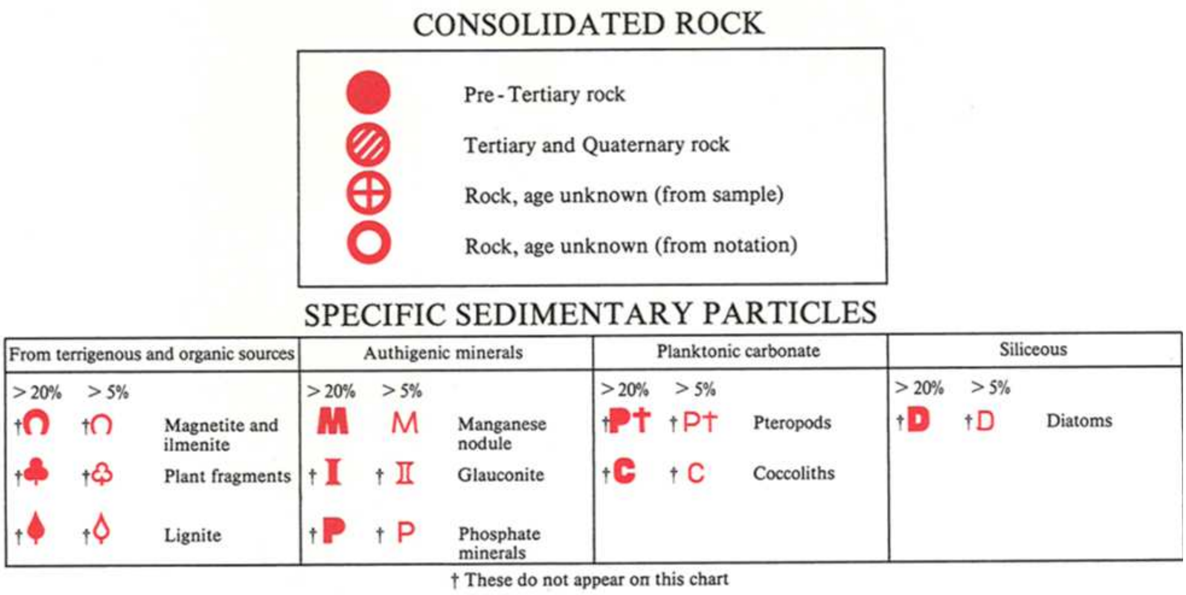

Figure 1.5: Example of specific notations used on Coastal Sediment charts, but not used in the present study.

Table 1.1: Summary table showing differences between the three different classification schemes used on each of the three different scales of NZ sediment charts, as depicted in Figures 1.1–1.5.

NZ Regional	Oceanic, Coastal (1965–70)		Coastal (post-1970)		
Sediment class	**Grain-size (mm)**	**Sediment class**	**Grain-size (mm)**	**Sediment class***	**Description**
Gravel/sand; calcareous gravel/sand	>256	Boulders	>2	Gravel	>30% gravel
	4–256	Cobbles & pebbles			
	0.5–4	Granules & coarse sand	0.064–2	Sand	>50% sand in <2 mm fraction; <30% gravel
Calcareous ooze; siliceous ooze	0.0625–0.5	Medium & fine sand			
Mud; deep ocean clays	<0.0625	Mud	0.064–0.004	Silt	>67% silt in mud fraction; <50% sand in <2 mm fraction
			<0.064	Mud	33–67% silt in mud fraction; <50% sand in <2 mm fraction
			<0.004	Clay	<33% silt in mud fraction; <50% sand in <2 mm fraction

* Also subdivided into <50% and >50% $CaCO_3$.

Sediment chart digitisation

Each of the charts from the Oceanic and Coastal sediment chart series was digitised on a digitiser board (Digipad 3648 L) using Tabletworks digitising and ArcGIS software, known as ArcMap. The following methodological approach was adopted for this process:

(1) The sediment chart was taped onto the digitiser board and the latitude and longitude of the bounding frames of the map (minimum x,y maximum x,y) noted.
(2) These coordinates were added as points in Arcmap. The northing and easting of these points were entered into a text file.
(3) The text file was loaded into Arcmap's digitiser settings, so that moving the digitising mouse on the digiboard will also move the mouse cursor on the computer screen with the correct projection.
(4) Digitising was achieved by tracing the outline of the sediment features shown on the map (using the digitising mouse), and simultaneously creating a digital copy on the computer at the correct projection.
(5) The sediment features were initially digitised as 'polylines' or vectors.
(6) Once completed, all the end points left by the polylines were joined together so there are no dangles and/or undershoots in the digitised lines.
(7) Arctoolbox was then used to transform the polylines into a polygon feature so that all the sediment features could be classified into their respective groups (i.e., sediment size, sediment type, etc, based on the classification schemes for each of the charts).

In contrast, the Regional sediment chart (Mitchell et al. 1989) was digitised on screen within ArcGIS using a rectified image, scanned at a scale of 1: 250 000, for visual interpretation of sediment class boundaries.

The digitised sediment charts in the Oceanic series were merged using an update tool to produce unique features that represent a single element combining Dominant and Sub-dominant classifications (see below). The same approach was adopted for the charts in the Coastal series. All Coastal datasets were combined into one layer where the most up-to-date chart data superseded the older chart. Neighbouring boundaries were re-drawn where required, though attribution of specific sediment classes across bounding charts were not changed where these were different (e.g., Oceanic charts Three Kings to Cook, and Coastal charts Patea to Cook Strait).

Where possible, all sample locations were attributed to the original data sources in terms of whether full or partial grain-size analyses were conducted, whether the initial classification was based on visual observations, or whether notations were taken from British Admiralty and/or New Zealand Hydrographic charts.

Polygon Attribution for Sediment Type

As discussed above, broadly speaking two different sediment classification interpretations have been used in the preparation of sediment distribution charts around New Zealand; one scheme based on a matrices-classification using compositional and grain-size data is used on charts published prior to 1989 (NZ Regional Sediments, Oceanic Series and early Coastal Series charts), and one using a ternary grain-size classification scheme used for those published after 1970 (most Coastal Series). Details of each of these schemes is presented below.

The NZ Regional Sediments 1: 6 000 000 chart (Mitchell et al. 1989), depicting sediments of the wider New Zealand region, sub-divides Sediment Type on the basis of mineralogical composition and/or origin (Terrigenous, Biogenic, Deep Ocean Clays, Volcanic, Authigenic) with Dominant and Sub-dominant types depicted, though exact proportions were not specified on the chart. The Terrigenous and Biogenic sediment components are further sub-divided on the basis of grain-size and/or composition with combined "Gravel/sand" and "Mud" in the Terrigenous component, and "Calcareous Gravel/sand", Calcareous ooze" and "Siliceous ooze" under the Biogenic sediment type.

Sediment classification in the Oceanic Series charts is separated into several sediment types based on mineral composition and/or particle origin (e.g., Terrigenous, Volcanic, Red Clay, Authigenic, Benthic Carbonate, Planktonic Carbonate, Siliceous). Each of these subdivisions is then divided into four-subcategories: Composition, Grain-size, Dominant and Subsidiary. While not stated on the charts, it is assumed that Dominant implies compositions greater than 50%, whereas Subsidiary indicates compositions greater than 20% (but supposedly less than 50%). For the older Coastal Series sediment charts (Foveaux, Mahia, Turnagain), a similar classification scheme was adopted, combining mineral compositional and grain-size information in a matrices-based format. Sediment types were Rock and Mineral Detritus, Organic Carbonate Remains and Foraminiferal Sediment with the same Dominant and Subsidiary designations across various grain-size classes, as adopted in the Oceanic Sediment chart series (Figure 1.3).

It was decided that the best way to capture the data in GIS from the NZ Regional Sediments and the Oceanic Sediment chart series was to have two polygon layers represented on each chart, namely 'Dominant' and 'Subsidiary'. Each digitised sediment feature polygon then had attributes describing what they contain and provided a sediment classification for that polygon (Table 1.2).

Table 1.2: Example of frequency of unique classification occurrence from the NZ Regional Sediments chart (Miscellaneous Chart Series No.67, Mitchell et al. 1989) where frequency refers to the number of times each classification was attributed on polygon features on the chart.

Frequency	Classification	Description
6	DOC	Deep Ocean Clays
12	G+S, t	Terrigenous Gravel/Sand
5	M, t	Terrigenous Mud
9	V	Volcanic
25	c-G+c-S, b	Biogenic Calc-Gravel/Calc-Mud
10	c-Ooze, b	Biogenic Calc-Ooze
1	c-g+c-s, t /c-Ooze, b	Terrigenous calc-gravel/calc-sand, Biogenic Calc-Ooze
2	c-ooze, b /DOC	Biogenic calc-ooze, Deep Ocean Clays
2	c-ooze, b /M, t	Biogenic calc-ooze, Terrigenous Mud
2	doc/c-Ooze, b	Deep ocean clays Terrigenous Calc-Ooze
3	g+s, t /M, t	Terrigenous gravel/sand, Terrigenous Mud
1	g+s, t /c-G+c-S, b	Terrigenous Gravel/sand Biogenic Calc-Gravel/Calc-Sand
3	m, t /G+S, t	Terrigenous muddy Terrigenous Gravel/Sand
1	si-Ooze, b	Biogenic Siliceous Ooze
3	si-ooze, b /DOC	Biogenic siliceous Deep Ocean Clays
1	v/DOC	Volcanic Deep Ocean Clays

Across the NZ Regional Sediments regional sediment chart and the Oceanic Sediment chart series, there are some differences that will affect interpretation and cross-referencing between the sediment distributions shown on the two different scale charts. In particular, Mitchell et al. (1989) combine gravel and sand in one category whereas the Oceanic charts distinguish between Boulders, Cobbles and Pebbles, Granules and coarse sand and Medium and fine sand. They also use a slightly different compositional scheme with Benthic and Planktonic carbonate sediments distinguished on the Oceanic chart series and not on the NZ Regional Sediments chart. The older Coastal sediment charts of Foveaux, Mahia, and Turnagain, while retaining the same grain-size classification as the Oceanic charts, did not distinguish between all of the same compositional classes, retaining a nominally "terrigenous" class (Rock and mineral detritus) and two "biogenic" classes (Organic carbonate remains and Foraminiferal sediment).

The sediment classifications used on the Coastal Sediment charts published after 1970 were completed using a ternary interpretation (modified from Folk 1965) with further compositional information provided by %$CaCO_3$. Under this scheme the dominant sediment was determined by its percentage contribution to the total grain-size distribution. For example, the dominant substrate constituent was Gravel if %gravel was greater than 30% of the total grain-size distribution, was Sand if %sand was greater than 50% in the less than 2 mm fraction, and, conversely, was Mud if %sand was less than 50% in the less than 2 mm fraction. The finer grain-sizes (sand and mud, < 2 mm) were further classified based on the %silt in the mud fraction with greater than 67% corresponding to a dominance of Silt, less than 33% silt indicating a Clay-dominated sediment, and 33–67% silt classified as Mud. Carbonate-dominated sediments were distinguished by having $CaCO_3$ percentages greater than 50%, leading to Calc-gravel, Calc-Sand and Calc-Mud designations. Correspondingly, sub-dominant carbonate contents were indicated where $\%CaCO_3$ was less than 50%. To enable consistency to be established with the Oceanic Sediment chart series, this scheme has been simplified into a classification that recognises Sediment Type, with subdivisions of Dominant and Subsidiary GIS layers.

As mentioned previously, Mahia, Turnagain, and Foveaux coastal sediment charts use a slight variant of the old classification system and an attempt has been made to revise the sediment attributions to be consistent with the ternary classification scheme used on newer charts. However, this approach means that on the digitised versions of the older charts the subdivision “Sand” may actually include coarser material in the lower end of the “Gravel” fraction because in the original classification scheme these features were classified as “Granule and coarse sand”. Thus, on the digitised versions of the Mahia, Turnagain, and Foveaux charts, features designated as “Sand” actually represent sediment dominated by grain-sizes from 4 mm to 0.063 mm (63 µm), rather than 2–0.063 mm as on the newer charts.

Similarly, the older Coastal Series charts characterised “Organic carbonate remains” and “Foraminiferal sediment” with Dominant subdivisions, which has been translated as similar to the category > 50% $CaCO_3$ on the newer charts, though it is uncertain what the exact proportion of calcium carbonate was on the older charts. Subsidiary carbonate sediments (< 50% $CaCO_3$) are also assumed to correspond to the > 20% subsidiary fraction designated on the older Coastal and Oceanic charts. This approach, however, is not without its flaws because the older classification schemes on the Foveaux, Turnagain, and Mahia sediment charts allow for the possibility of classifications such as “calc-sandy Sand” and “gravelly calc-Gravel” that are totally inconsistent with the more recent Coastal charts. In the older cases, the un-prefixed component corresponds to the terrigenous, inorganic component while the “calc” prefix indicates a dominance or sub-dominance of carbonate material of a particular grain-size.

To gain some consistency across all of the Coastal charts, therefore, only 1 or 2-class subdivisions were used for the digitised versions of the Foveaux, Turnagain, and Mahia sediment charts, such that a polygon designated as “muddy calc-sandy Sand” based on the original chart is shown as “muddy Sand” on the new digitised version. Similarly, sediment polygons designated as “sandy calc-Sand” based on the original classification are shown as “calc-Sand” on the digitised chart. Obviously, this introduces substantial differences between the original sediment classifications used on the older charts and in some situations may not reflect the “true” sediment classification type for each polygon. These discrepancies are most noticeable on the Foveaux chart (Cullen & Gibb 1965) where there is a multitude of sediments comprising mixtures of grain-sizes and compositions. Without further grain-size analyses and re-interpretations of the historical data, there is effectively no other way in which an internally consistent classification scheme for the Coastal Sediments chart series could be generated for the purposes of the present study. Hence, the classification scheme, incorporating both compositional and grain-size information, as used on the older Coastal charts was retained for these specific charts.

Median grain-size attributes

In order for the GIS data to be useful for input into the NIWA Wave Model (WAM, Gorman et al. 2003a, b), each of the sediment feature polygons were ascribed a median grain-size. This was determined empirically by deriving “ideal” grain-size distributions based on the sediment type attribution for each polygon, taking into account the relative dominance of the attributed grain-size categories. Median grain-sizes were then derived from these “ideal” distributions.

It should be noted that given the often heterogeneous nature of seafloor sediments, the concept of a median grain-size is potentially meaningless and at worst erroneous, especially in continental margin, shelf, and coastal settings. For example, in muddy sandy gravels, which constitute a common sediment category in such settings, the total grain-size distribution may be essentially bi-modal in nature. However, since the gravel component dominates the total grain-size distribution by comprising at least more than 30% of the total grain-size distribution, the finer grain-sizes will not be represented adequately by a specific median (or mean) grain-size despite being important constituents of the sediment.

The median grain-size concept also does not account for preferential resuspension of individual constituents of the sediment by wave action or other seabed currents (i.e., tides, longshore drift, rips). For muddy sandy gravels, the coarsest fraction by virtue of its size and density, and perhaps the more cohesive finest fractions, are likely to be less mobile than the sandier component. Similarly, different classes of carbonate-rich sediments will be affected variably by currents depending on the composition of the carbonate material.

Meta-data, quality assurance and quality control processes

All digitised sediment charts were cross-checked with the original charts to ensure accuracy with the original data and continuity across the entire dataset. As mentioned previously, however, discrepancies will still occur across chart boundaries due to the different sediment classification schemes adopted by different chart types (i.e., Oceanic v Coastal) and different chart ages (e.g., Coastal Series charts of Cook Strait v Patea). No attempt has been made to reconcile differences in the geographical depiction of sediment boundaries across different charts.

References

Arron, E.S. (1986). Oamaru Coastal Sediments chart (1: 200 000). New Zealand Oceanographic Institute (now NIWA), Department of Scientific and Industrial Research, Wellington, New Zealand.

Arron, E.S.; Doyle, A.C. (1983). Mokau Coastal Sediments chart (1: 200 000). New Zealand Oceanographic Institute (now NIWA), Department of Scientific and Industrial Research, Wellington, New Zealand.

Carter, L.; Eade, J.V. (1980). Hauraki Coastal Sediments chart (1: 200 000). New Zealand Oceanographic Institute (now NIWA), Department of Scientific and Industrial Research, Wellington, New Zealand.

Carter, L.; Herzer, R.H. (1986). Pegasus Coastal Sediments chart (1: 200 000) (2nd Edition). New Zealand Oceanographic Institute (now NIWA), Department of Scientific and Industrial Research, Wellington, New Zealand.

Cullen, D.J.; Gibb, J.G. (1965). Foveaux Coastal Sediments chart (1: 200 000). New Zealand Oceanographic Institute (now NIWA), Department of Scientific and Industrial Research, Wellington, New Zealand.

Doyle, A.C.; Arron, E.S. (1982). Raglan Coastal Sediments chart (1: 200 000). New Zealand Oceanographic Institute (now NIWA), Department of Scientific and Industrial Research, Wellington, New Zealand.

Doyle, A.C.; Carter, L.; Glasby, G.P.; Lewis, K.B. (1979). Bay of Plenty Coastal Sediments chart (1: 200 000). New Zealand Oceanographic Institute (now NIWA), Department of Scientific and Industrial Research, Wellington, New Zealand.

Eade, J.V. (1974). Poor Knights Coastal Sediments chart (1: 200 000). New Zealand Oceanographic Institute (now NIWA), Department of Scientific and Industrial Research, Wellington, New Zealand.

Folk, R.L. (1965). Petrology of Sedimentary Rocks. Hemphills, Texas: 159p.

Gorman, R.M.; Bryan, K.R.; Laing, A.K. (2003a). Wave hindcast for the New Zealand region: nearshore validation and coastal wave climate. *New Zealand Journal of Marine and Freshwater Research 37*: 567–588.

Gorman, R.M.; Bryan, K.R.; Laing, A.K. (2003b). Wave hindcast for the New Zealand region: deep-water wave climate. *New Zealand Journal of Marine and Freshwater Research 37*: 589–612.

Herzer, R.H. (1979). Banks Coastal Sediments chart (1: 200 000). New Zealand Oceanographic Institute (now NIWA), Department of Scientific and Industrial Research, Wellington, New Zealand.

Herzer, R.H. (1981). Ellesmere Coastal Sediments chart (1: 200 000). New Zealand Oceanographic Institute (now NIWA), Department of Scientific and Industrial Research, Wellington, New Zealand.

Lewis, K.B.; Gibb, J.G. (1970). Turnagain Coastal Sediments chart (1: 200 000). New Zealand Oceanographic Institute (now NIWA), Department of Scientific and Industrial Research, Wellington, New Zealand.

Lewis, K.B.; Mitchell, J.S. (1980). Cook Strait Coastal Sediments chart (1: 200 000). New Zealand Oceanographic Institute (now NIWA), Department of Scientific and Industrial Research, Wellington, New Zealand.
McDougall, J.C. (1975). Cook Oceanic Sediments chart (1: 1 000 000). New Zealand Oceanographic Institute (now NIWA), Department of Scientific and Industrial Research, Wellington, New Zealand.
McDougall, J.C. (1979). Three Kings Oceanic Sediments chart (1: 1 000 000). New Zealand Oceanographic Institute (now NIWA), Department of Scientific and Industrial Research, Wellington, New Zealand.
McDougall, J.C. (1982). Bounty Oceanic Sediments chart (1: 1 000 000). New Zealand Oceanographic Institute (now NIWA), Department of Scientific and Industrial Research, Wellington, New Zealand.
Mitchell, J.S. (1987). Tasman Coastal Sediments chart (1: 200 000). New Zealand Oceanographic Institute (now NIWA), Department of Scientific and Industrial Research, Wellington, New Zealand.
Mitchell, J.S.; Carter, L.; McDougall, J.C. (1989). New Zealand Regional Sediments (1:6 000 000). New Zealand Oceanographic Institute (now NIWA), Department of Scientific and Industrial Research, Wellington, New Zealand. NZOI Miscellaneous Chart Series 67.
Nodder, S.D.; Edwards, N.A.; Burrows, M.W. (1992). Patea Coastal Sediments chart (1: 200 000) (2nd Edition). New Zealand Oceanographic Institute (now NIWA), Department of Scientific and Industrial Research, Wellington, New Zealand.
Pantin, H.M.; Gibb, J.G. (1968). Mahia Coastal Sediments chart (1: 200 000). New Zealand Oceanographic Institute (now NIWA), Department of Scientific and Industrial Research, Wellington, New Zealand.
Snelder, T.H.; Leathwick, J.R.; Dey, K.L.; Rowden, A.A.; Weatherhead, M.A.; Fenwick, G.D.; Francis, M.P.; Gorman, R.M.; Grieve, J.M.; Hadfield, M.G.; Hewitt, J.E.; Richardson, K.M.; Uddstrom, M.J.; Zeldis, J.R. (2006). Development of an ecologic marine classification in the New Zealand region. *Environmental Management 39 (1)*: 12–29. DOI: 10.1007/s00267-005-0206-2.

APPENDIX 2: SEDIMENT DISTURBANCE/RESUSPENSION DATA SUMMARY

Prepared by Richard Gorman.

Directories:

00_all	Averages over the full hindcast period (all years, all months)
MM_mmm	Monthly averages, i.e. all data within a single month, all years MM = 01-12, mmm = Jan,..., Dec

Files:

*.grd files are ASCII grid files with a 6-line header, intended to ready for GIS import.
The header is:

ncols	1401
nrows	1281
xllcorner	157.5
yllcorner	-57
cellsize	0.025
nodata_value	(-9 or -20)

longitude.grd	Longitudes of the output grid cells (WGS-84)
latitude.grd	Latitudes of the output grid cells (WGS-84)
grainsizeD.grd	Median grainsize (mm) at each grid cell used in the analysis
Hsmean_DallMM.grd	Average of significant wave height (m)
Fpmean_DallMM.grd	Average of peak wave period (s)
Fxmean_DallMM.grd	Average of x-component of wave energy flux (kW/m)
Fymean_DallMM.grd	Average of y-component of wave energy flux (kW/m)
Fmagmean_DallMM.grd	Average of magnitude of wave energy flux (kW/m)
UBMS_DallMM.grd	log10(Average of mean-square bed orbital velocity (m2/s2))
USTAR_DallMM.grd	log10(Average of friction velocity (m/s))
URAT_DallMM.grd	log10(Average of the ratio of friction velocity to the critical friction velocity for entrainment)
SEDM_DallMM.grd	log10(Average of the fraction of time for which the entrainment threshold is exceeded)
FCmeansDMM.mat	Matlab MAT-file containing all of the above arrays

Methods:

Wave model outputs were taken from the NIWA WAM forecast system, running on a lat/lon grid of longitudes 105°–220° E at resolution 1.25 degrees, and latitudes 78° S – 0° at resolution 1.0 degrees. Outputs are available at 3-hourly intervals (apart from some gaps). Since February 1997, analysis includes summary wave statistics (significant wave height, mean and peak period, mean and peak direction, etc.) on the whole model domain, and full directional spectra at cells near the NZ coast.

The program *fluxinterp8* was used to interpolate hindcast spectra to finer spatial resolution, using a method that takes account of blocking of wave propagation by land at sub-grid scales. The full output grid covered:
longitudes 157.5° to 192.5° at 0.025 degree resolution
latitudes -57.0° to -25.0° at 0.025 degree resolution

Due to memory and runtime limits, the *fluxinterp8* program was run on two domains:
1. full domain at low resolution: longitudes 157.5° to 192.5° at 0.125 degree resolution; latitudes -57.0° to -25.0° at 0.1 degree resolution
2. sub-domain covering main NZ islands at highest resolution: longitudes 165.0° to 180.0° at 0.025 degree resolution; latitudes -49.0° to -33.0° at 0.025 degree resolution

Time-averages from the two domains were merged at the end, using simple bilinear interpolation where necessary.

At each time step, mean-square bed orbital velocities were derived from the spatially-interpolated wave spectra. From the RMS bed-orbital velocity (UBED), a friction velocity was derived with a friction coefficient derived using the Swart formula, i.e.,

```
X = 2.5*DIAM*TPI*FREQ/UBED
FW = EXP(5.213*X**0.194 - 5.977)
USWART = UBED*SQRT(0.5*FW)
```

Critical values of the friction velocity were derived from the median grain size using Yalin's empirical relationship.

APPENDIX 3: CARBONATE PARAMETERS FROM THE GLODAP DATA BASE FOR THE NEW ZEALAND EEZ.

Prepared by Kim Currie.

Total alkalinity (A_T), potential alkalinity (A_P), and dissolved inorganic carbon concentration (C_T)
Values for A_T, A_P and C_T were extracted from the GLODAP database (http://cdiac.ornl.gov/oceans/glodap/Glodap_home.htm, (Key et al. 2004)) using the LAS facility for the area 157° E – 167° W and 57°–24° S in 1° x 1° bins at the following depths: 0, 10, 20, 30, 50, 75, 100, 125, 150, 200, 250, 300, 400, 500, 600, 700, 800, 900, 1000, 1100, 1200, 1300, 1400, 1500, 1750, 2000, 2500, 3000, 3500, 4000, 4500, 5000, 5500 m.

Aragonite Saturation
The value given is the aragonite saturation index, Ω_a, defined as:

$$\Omega_a = \frac{[Ca^{2+}][CO_3^{2-}]}{K'_{sp}}$$

where $[Ca^{2+}]$ and $[CO_3^{2-}]$ are the concentrations of calcium ion, and carbonate ion respectively and K'_{sp} is the stoichiometric solubility product for the dissolution reaction

$$CaCO_{3(a)} \leftrightarrow Ca^{2+}_{(aq)} + CO_3^{2-}{}_{(aq)}$$

Ω_a is calculated from the salinity, temperature, depth (pressure), total alkalinity and total dissolved inorganic carbon concentration.

Temperature and salinity data (long term annual means, derived from data for years 1900–97) were extracted from the National Oceanographic Data Centre (NODC, Levitus) World Ocean Atlas Data 1998 database (NODC_WOA98 data provided by the NOAA/OAR/ESRL PSD, Boulder, Colorado, USA, from their Web site at http://www.cdc.noaa.gov/) for the same area and depth bins as the carbonate parameters.

The constants of Mehrbach et al. (1973) were used for the carbonate speciation calculation, and the aragonite solubility product, K'_{sp}, was determined using the Millero (1995) algorithm. The calcium ion concentration ($[Ca^{2+}]$) was determined from salinity using the expression

$$[Ca^{2+}] = 0.01028 \times \frac{S}{35}$$

where S is the salinity. The calculation was performed using the computer programme swco2 (http://neon.otago.ac.nz/chemistry/research/mfc/people/keith_hunter/software/swco2/swco2.htm).

For supersaturated water Ω_a is greater than 1, and for undersaturated water Ω_a is less than 1. Aragonite deposited on the sea floor is stable with respect to dissolution if the overlying seawater is supersaturated ($\Omega_a > 1$).

References

Key, R.M.; Kozyr, A.; Sabine, C.L.; Lee, K.; Wanninkhof, R.; Bullister, J.; Feely, R.A.; Millero, R.; Mordy, C.; Peng, T.-H. (2004). A global ocean carbon climatology: Results from GLODAP. *Global Biogeochemical Cycles 18* (CB4031).

Mehrbach, C.; Culberson, C.H.; Hawley, J.E.; Pytkowicz, R.M. (1973). Measurement of the apparent dissociation constants of carbonic acid in seawater at atmospheric pressure. *Limnology and Oceanography 19 (6)*: 897–907.

Millero, F.J. (1995). Thermodynamics of the carbon dioxide system in the oceans. *Geochimica et Cosmochimica Acta 59 (4)*: 661–677.

APPENDIX 4: PRIMARY PRODUCTIVITY

Prepared by Matt Pinkerton.

1.0 Introduction

There is considerable international and New Zealand interest in net oceanic primary production (NPP) for understanding ecosystem dynamics and carbon cycling. The spatial and temporal variability of marine photosynthesis is poorly understood observationally. Only isolated snapshots are available via ship-based sampling and it is impossible to quantify basin-scale primary productivity from in situ measurements alone. Relatively recently (within the last decade) methods have been developed to use satellite observations of the ocean for long-term, large-area estimates of NPP for all the world's oceans.

Satellite observations now routinely provide global estimates of (amongst others) surface chlorophyll concentration (Chl), photosynthetically available radiation (PAR), and sea surface temperature (SST). These data can be combined to estimate NPP. Given that validation data for NPP around New Zealand is relatively scarce, and that there are many alternative NPP algorithms available, we consider and compare three of the most widely used formulations.

The original empirical models of NPP (e.g., Platt 1986) have been superseded by simple mechanistic models based on satellite observations of chlorophyll concentration, incident light, and a yield function which incorporates the physiological response of the phytoplankton to light, nutrients, temperature and other environmental variables. SST is often used to parameterise this yield function. A range of such modelling approaches exist (e.g., Platt & Sathyendranath 1993; Longhurst et al. 1995; Howard & Yoder 1997; Antoine & Morel 1996a, 1996b; Behrenfeld & Falkowski 1997b; Ondrusek et al. 2001), which are distinguished by the degree of integration over depth and irradiance, and the manner in which temperature is used to parameterise the photosynthetic yield function (Behrenfeld & Falkowski 1997a). We consider two such approaches here, which are described in detail below. We also consider a new approach, based on satellite-observed carbon rather than chlorophyll, which takes advantage of more recent developments in inherent optical property retrievals from ocean colour instruments, and the realisation that there might be important information on phytoplankton physiological state in these measurements — The carbon-based ocean production model (Behrenfeld et al. 2005, Siegel et al. 2005, Westberry et al. 2008).

2.0 Methods

Data and algorithms were sourced from the Oregon State University "Ocean Productivity" project (web.science.oregonstate.edu/ocean.productivity). Estimates of net primary production (NPP) are obtained at monthly resolution, in units of mgC m^{-2} d^{-1}. Online products were provided as 1080x2160 global grids in hdf format. Months were combined using log-averaging. The spatial resolution is 10' in latitude and longitude, which equates to a resolution of approximately 18.6 km (latitude) and 12–16 km (longitude) for the New Zealand EEZ. (The resolution of the CbPM product seems worse than this because it relies on mixed layer depth obtained from a number of global circulation models which are available only at a coarser resolution of between 0.25°–1°.)

Three processing algorithms are considered. All three algorithms rely significantly on measurements of ocean colour (visible band, multispectral, normalized water-leaving radiance) by radiometers on polar Earth-orbiting satellites. Two sets of ocean colour data are available: SeaWiFS (NASA-OrbImage Sea Viewing Wide Field-of-view Sensor: oceancolor.gsfc.nasa.gov/SeaWiFS), and MODIS-Aqua (NASA Moderate Resolution Imaging Spectroradiometer: modis.gsfc.nasa.gov). Both the VGPM and Eppley-VGPM models were applied to data from both the SeaWiFS and MODIS sensors. The CBPM has only been applied to data from the SeaWiFS at present. In all cases, incident Photosynthetically Active Radiation (PAR) data were estimated based on data from the SeaWiFS sensor. Euphotic depths in all models were calculated using the same chlorophyll-based model of Morel & Berthon (1989).

2.1. Standard-VGPM algorithm ("VGPM")

The standard Vertically Generalized Production Model (VGPM) (Behrenfeld & Falkowski 1997a) is a chlorophyll-based model that estimates NPP from chlorophyll using a temperature-dependent description of chlorophyll-specific photosynthetic efficiency. For the VGPM, net primary production is a function of chlorophyll, available light, and the photosynthetic efficiency.

2.2. Eppley-VGPM algorithm ("Eppley")

The Eppley-VGPM model differs from the Standard VGPM only in the use of an exponential temperature-dependent description of photosynthetic efficiencies (Eppley 1972). While Eppley's analysis has no direct relationship to the description of average photosynthetic efficiencies, its application in ocean productivity models is commonplace. The exact "Eppley-function" used in the VGPM is based on the productivity model of Morel (1991).

2.3. Carbon-based Production Model ("CbPM")

The carbon-based ocean production model (Behrenfeld et al. 2005; Westberry et al. 2008) is based on the observation that estimation of NPP using chlorophyll and temperature-based models rely on yield terms that are empirical descriptions of physiological variability and often perform poorly when compared to local field measurements. Two recent advances have facilitated this new approach to estimating NPP from space.

First, the inherent optical properties (IOPs) of phytoplankton (absorption and scattering coefficients) change depending on their physiological condition. Inherent optical properties hence carry information that can be useful in estimating primary productivity rates of phytoplankton. Behrenfeld & Boss (2003) demonstrated a first-order correspondence between $Chl{:}c_p$ (c_p=beam attenuation ratio at 660 nm) and ^{14}C-tracer measure of phytoplankton physiological condition. This can be interpreted as phytoplankton responding to changes in light, nutrients, and temperature by adjusting cellular pigment levels to match the new demands for photosynthesis (Behrenfeld et al. 2005). In waters where the attenuation is dominated by phytoplankton (Case 1 waters), total particulate carbon concentration was found to covary with light scattering properties (DuRand & Olsen 1996, Stramski et al. 1999, Loisel et al. 2001, Behrenfeld & Boss 2003, 2006, Green et al. 2003, Green & Sosik 2004).

Second, in Case 1 (open ocean) waters, methods have been developed to estimate both *Chl* and *C* from satellite measurement of ocean colour (e.g. Garver & Siegel 1997, Lee et al. 2002, Maritorena et al. 2002, Siegel et al. 2002, Pinkerton et al. 2006). The satellite-derived estimates of chlorophyll concentration and carbon concentration are henceforth termed Chl_{sat} and C_{sat}. A number of different algorithms to estimate IOPs from ocean colour satellite data are available. The algorithm used here uses the Garver-Siegel-Maritorena spectral matching algorithms (Garver & Siegel 1997) applied to SeaWiFS measurement to simultaneously retrieve information on particulate backscattering scattering coefficients, phytoplankton pigment absorption, and coloured dissolved organic carbon absorption. Analysis of the resultant global $Chl_{sat}{:}C_{sat}$ data revealed seasonal patterns consistent with regional ecology, strong dependencies on mixed layer light levels that were consistent with laboratory studies, and relations between Chl_{sat} and both SST and nutrient stress that were also consistent with laboratory studies. Behrenfeld et al. (2005) argued that these results demonstrate that the link between $Chl_{sat}{:}C_{sat}$ and algal physiology, and therefore growth rates, can be used in a global NPP algorithm.

Combining these advances led to the development of a method for estimating NPP in terms of the product of carbon biomass and growth rate, rather than the traditional product of chlorophyll and photosynthetic efficiencies. Of significance is the fact that unlike chlorophyll-based models, most of the key components of the new CbPM approach are potential satellite observables. Ocean mixed layer depth is typically taken from a relatively coarse resolution climatology based on dynamic modelling of the upper ocean. The data source for mixed layer depth varies between 1997 and 2006, depending of quality and availability. Data sources include Thermal Ocean Prediction Model from US Navy Fleet Numerical Meteorology and Oceanography Center, and Simple Ocean Data Assimilation, and the

"Simple Ocean Data Assimilation" project (Carton et al. 2000a,b). Results based on CbPM are only available based on the SeaWiFS data at present.

2.4 Climatological analysis, and remapping

Climatological averages of each product were obtained by log-averaging non-error pixels over the period of data availability. Only data based on SeaWiFS data were used to generate the climatological averages because the dataset based on MODIS observations is far shorter at present. Data were then remapped onto a Mercator Projection with a mapped average resolution of approximately 1 km. Data are provided for the Marine Environment Classification (MEC) domain bounded by the following coordinates: 24°–57.5°S 157°E–167°W. A spline smooth was used to interpolate between data points. Data were output in ASCII format as required by the scheme.

3.0 Results

Figure 4.1 shows the intercomparison between the median value of NPP from the algorithms considered over the New Zealand EEZ. Figures 4.1a and b show that the effect of different ocean colour satellite data sources (SeaWiFS and MODIS) is small at the New Zealand EEZ level. Significant effort has been expended by the international remote-sensing science community (and by NASA in particular) at providing a consistent time series of ocean colour observations between sensors, so this result is reassuring. Figure 4.1c and Figures 4.2–4.4 show that there are large differences between the estimates of NPP around New Zealand by the three algorithms, though they all capture the strong annual seasonality in NPP around New Zealand. NPP peaks in the late-spring/early summer (December–January) and has an annual minimum in the late winter (July–August). The VGPM model suggests that the phase of NPP is about a month earlier than the CbPM and Eppley models show. NPP by the CbPM model has the largest dynamic range seasonally, and also the highest maximum values of NPP. The Eppley model has the smallest seasonal range, and also estimates the lowest maximum production values. The VGPM model gives almost the same maximum NPP values as CbPM, but significantly higher annual minimum values.

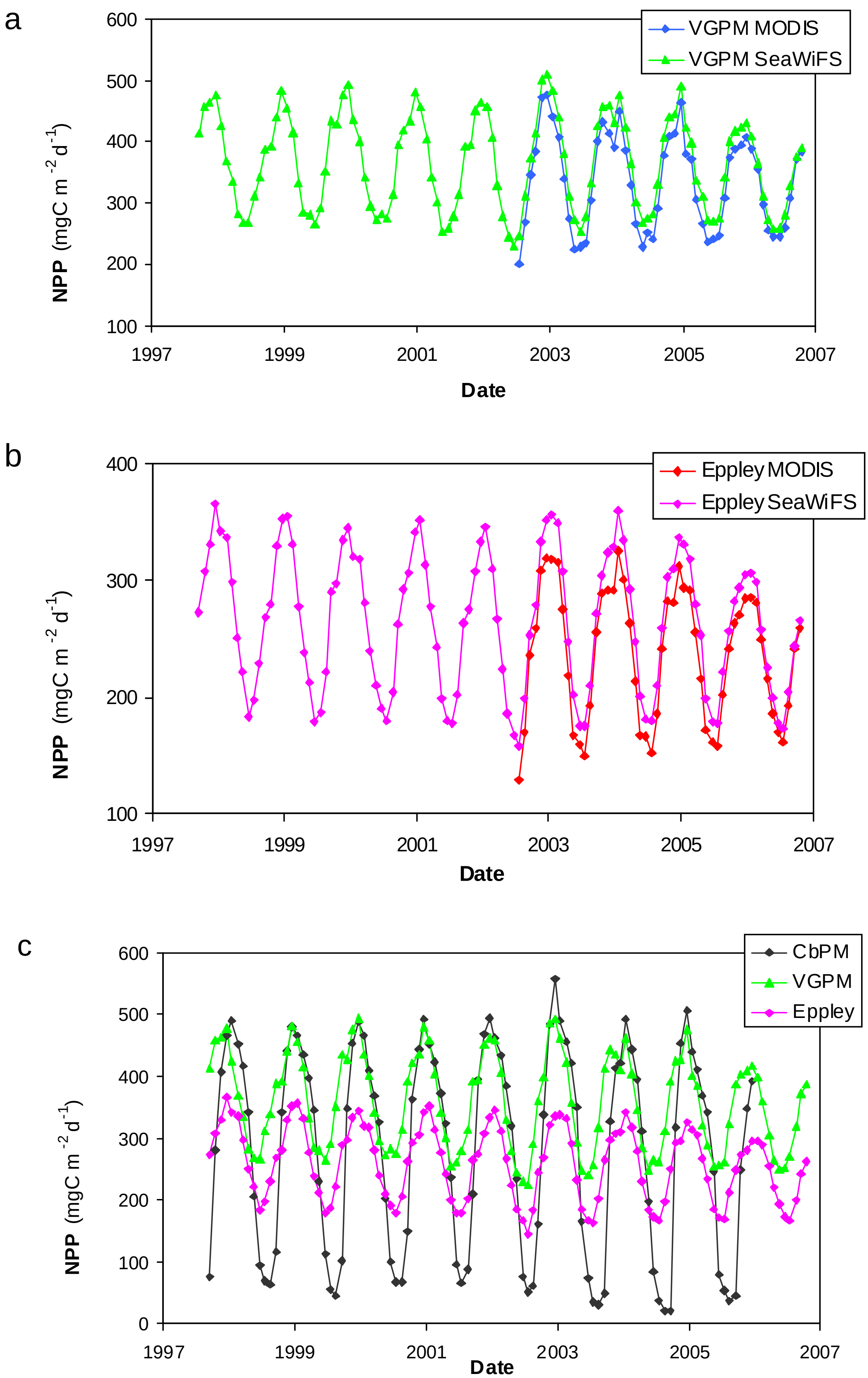

Figure 4.1: Net Primary Production (NPP) estimates from three algorithms (CbPM, VGPM, Eppley) based on two sets of ocean colour data (MODIS, SeaWiFS). a: Effect of different ocean colour data on VGPM model. b: Effect of different sources of ocean colour data on Eppley model. c: Comparison between three algorithms.

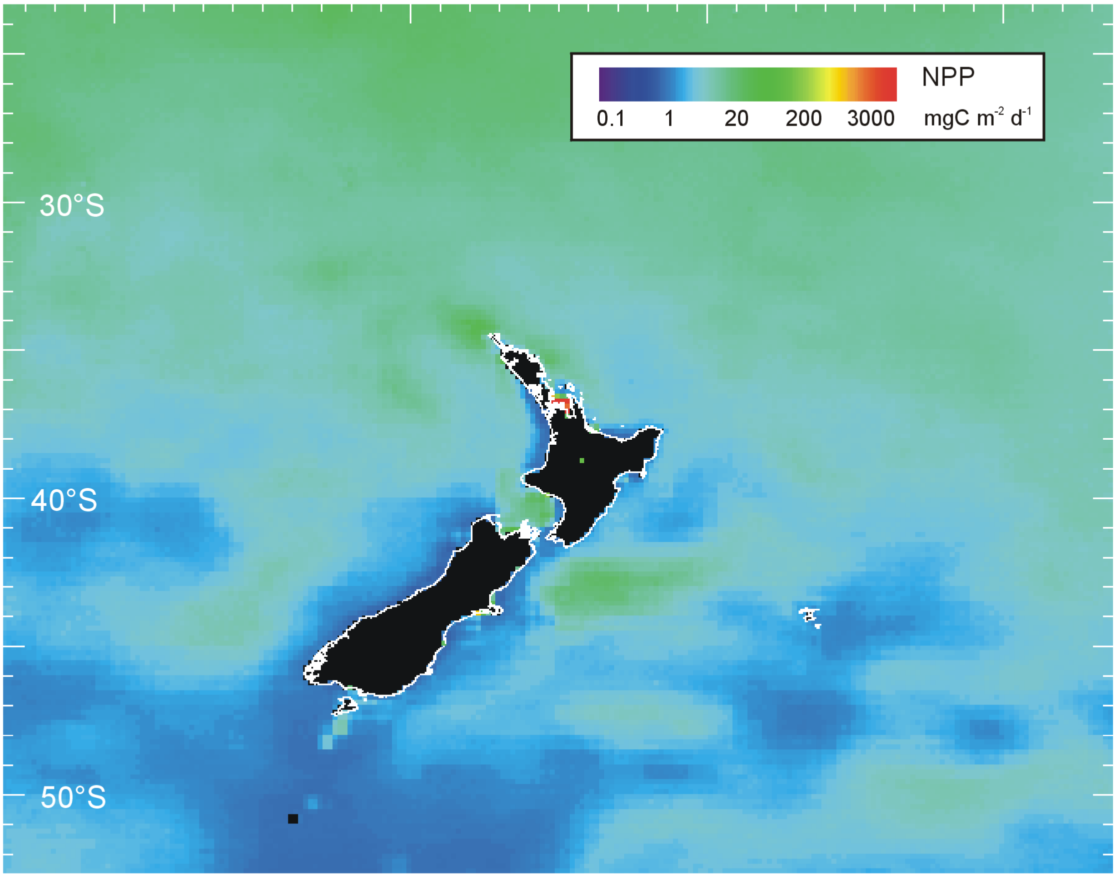

Figure 4.2: Climatology of Net Primary Production (NPP) estimates from CbPM model (SeaWiFS data) for period 1997–2005. Note the large amount of pixilation compared to the other two models. This is a result of the coarse-resolution mixed layer depth data (0.25° at best). The mixed-layer depth product is used only in this algorithm.

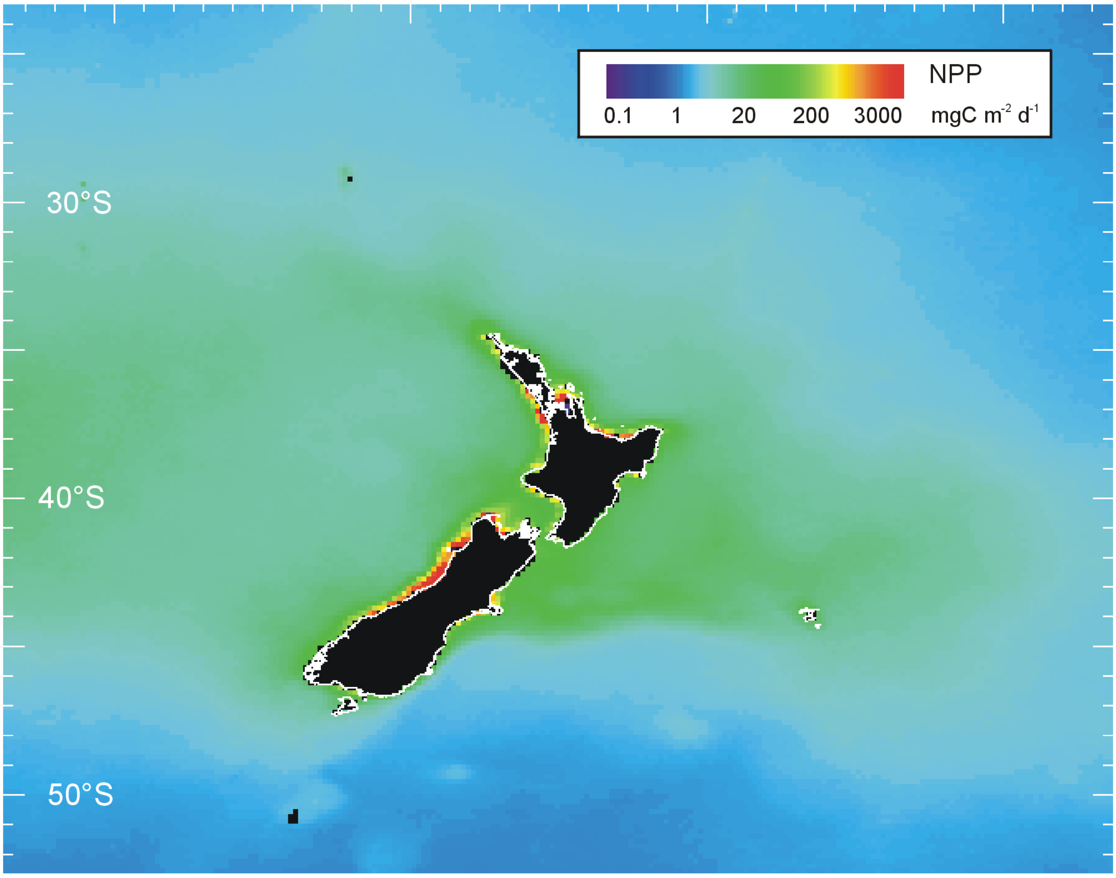

Figure 4.3: Climatology of Net Primary Production (NPP) estimates from VGPM model (SeaWiFS data) for period 1997–2006.

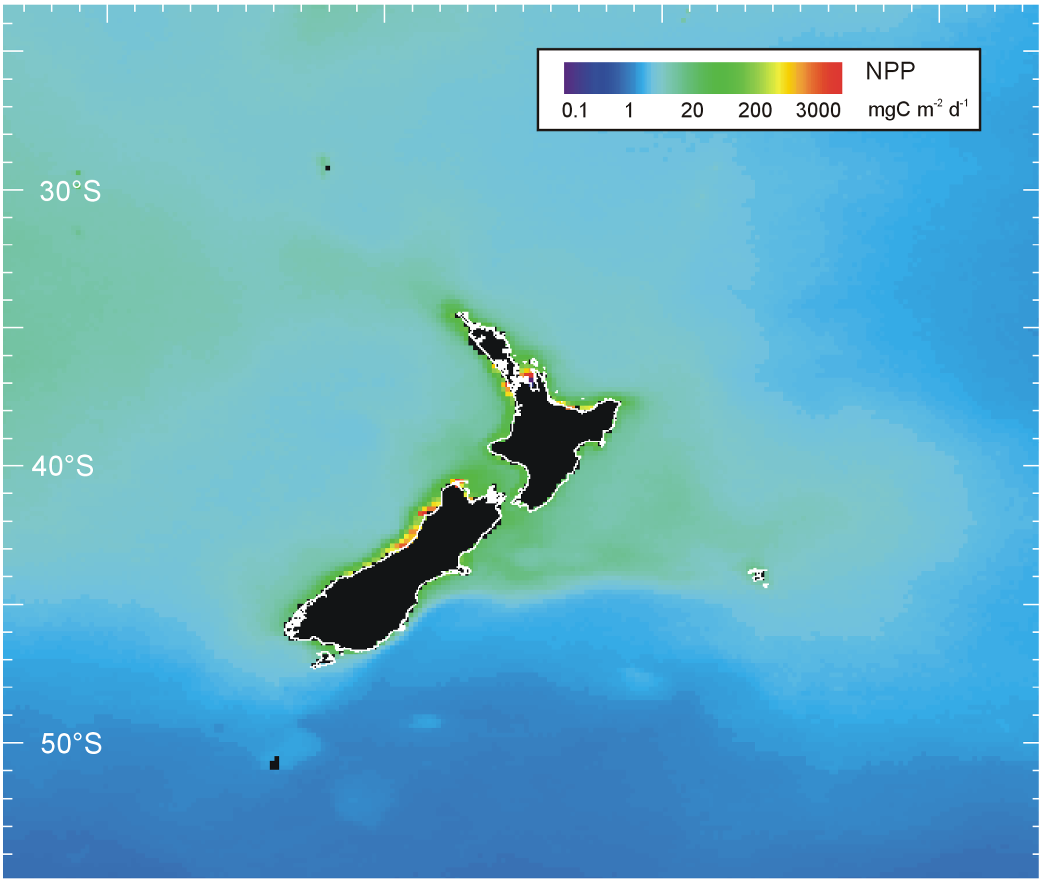

Figure 4.4: Climatology of Net Primary Production (NPP) estimates from Eppley model (SeaWiFS data) for period 1997–2006.

4. Discussion

Global comparisons between these three models show broad qualitative agreement, but with significant differences quantitatively and regionally. Campbell et al. (2002) summarised the second primary production "round-robin" experiment which used in situ ^{14}C uptake measurements from 89 stations around the world to test the ability of 12 chlorophyll-based models developed by 10 teams to predict depth-integrated NPP. The study showed that 7 of the 12 models were typically within a factor of 2 of the ^{14}C measurements, with algorithms performing best in the Atlantic region, and performing worst in the equatorial Pacific and Southern Oceans. Campbell et al. (2002) suggested that this might be caused by a high dynamic NPP range in the Southern Ocean, and high-nitrate low-chlorophyll (HNLC) conditions in the equatorial Pacific and Southern Ocean. HNLC conditions are poorly addressed by all algorithms.

More recent work as part of the third primary production "round robin" experiment (Carr et al. 2006) aimed to identify conditions under which 24 candidate NPP models agreed or disagreed. A cluster analysis on the model pair-wise correlation matrix was used to identify groups which respond similarly to environmental conditions or regions. The groups were used to define a mean model which, while not necessarily representing "reality", is useful as a comparative reference. The range of model NPP estimates is large relative to the mean, particularly in the Southern Ocean and in subantarctic waters.

The most difficult conditions for chlorophyll-based models near New Zealand are HNLC, low-temperature, and high chlorophyll conditions (Carr et al. 2006), which occur south of the subtropical front in the New Zealand EEZ. Carr et al. (2006) suggested that research to improve NPP accuracy should aim to combine remotely-sensed variables with historic or modelled information linked to geography, biome, or regime – i.e., local knowledge of the region is important. Similarly, the CbPM approach is not likely to work well in HNLC waters because the laboratory and field data used to parameterise the model do not include the special physiological conditions that exist in these regions. In particular, when iron limits NPP, phytoplankton physiology can change in ways that invalidate some of the assumptions and parameterisations used by CbPM.

Spatially, the models suggest high climatological average NPP values along the west coast and in the Hauraki Gulf, and generally close to the New Zealand coast. These values should be treated with caution because all three algorithms are strictly applicable only to the open ocean. Satellite measurements of chlorophyll (SeaWiFS and MODIS) and inherent optical properties using the Garver-Siegel-Maritorena algorithm are unreliable in the coastal zone. High overestimates of chlorophyll can occur here due to co-occurring suspended sediment and dissolved coloured organic matter from land run-off ("yellow-substance"). These will tend to lead to overestimates of NPP in the coastal zone. Also, algal growth physiology in the coastal zone does not necessarily follow the same relationships as in the open ocean, because nutrient supply and vertical mixing can be substantially different. The NPP values around the New Zealand coast in these data should hence be treated with scepticism.

The general structure of climatological average NPP shown in the open ocean in Figures 4.3 and 4.4 (VGPM and Eppley models) appear reasonable. We would expect higher production east and west of New Zealand in subtropical waters, especially around the Subtropical Front to the east. NPP in subantarctic waters (south of New Zealand) and tropical waters (north of New Zealand) is thought to be lower on average than in subtropical waters. The patchiness in NPP from the CbPM in subantarctic waters is unlikely to be real. As mentioned, none of the models estimate NPP in these HNLC waters adequately, and it is possible that the CbPM model is more sensitive to these inadequacies than the other two formulations.

5. Conclusions and recommendations

While it is clear from these comparisons that substantial quantitative differences exist between various NPP algorithms and products, the spatial and seasonal patterns are qualitatively similar. At present, we cannot recommend the "best" algorithm to use. We reiterate that resources are being devoted to validate and improve the accuracy of NPP products internationally and at NIWA within the 12-year FRST (Foundation for Research Science and Technology) Coasts and Oceans OBI (Outcome Based Investment) project. In the interim, if one product alone is to be used, we would suggest that the Standard-VGPM algorithm ("VGPM") product based on SeaWiFS data be preferred.

6. Acknowledgements

Remapping and output was carried out by Dr Ude Shankar (NIWA Christchurch). Dr Ken Richardson (NIWA Wellington) carried out much of the literature review of primary productivity algorithms leading to this report. Data used courtesy of Oregon State University "Ocean Productivity" project. SeaWiFS data used courtesy of NASA and OrbImage Inc. MODIS data used courtesy of NASA. Funding for this work was provided by Ministry of Fisheries Benthic Optimised MEC project (BEN2006/01, Obj 5). This work relies significantly on funding from the Foundation for Research, Science and Technology project (capability fund project CRCM063: "Bio-optical properties and productivity algorithms", and "Ocean Ecosystems: Their Contribution to New Zealand Marine Productivity" C01X0223).

7. References

Antoine, D; Morel, A. (1996a). Oceanic primary production 1: Adaptation of a spectral light-photosynthesis model in view of application to satellite chlorophyll observations. *Global Biogeochemical Cycles 10*: 43–55.

Antoine, D.; Morel, A. (1996b). Oceanic primary production 2: Estimation of global scale from satellite (Coastal Zone Color Scanner) chlorophyll. *Global Biogeochemical Cycles 10*: 57–69.

Behrenfeld, M.J.; Boss, E. (2003). The beam attenuation to chlorophyll ratio: An optical index of phytoplankton physiology in the surface ocean*? Deep-Sea Research I (50)*: 1537–1549.

Behrenfeld, M.J.; Boss, E. (2006). Beam attenuation and chlorophyll concentration as alternative optical indices of phytoplankton biomass. *J. Marine Research 64*: 431–451.

Behrenfeld, M.J.; Boss, E.; Siegel, D.A.; Shea, D.M. (2005). Carbon-based ocean productivity and phytoplankton physiology from space. *Global Biogeochemical Cycles* GB1006, DOI:10:1029/2004GB002299.

Behrenfeld, M.J.; Falkowski, P. (1997a). A consumer's guide to phytoplankton primary productivity models. *Limnology & Oceanography 42(7)*: 1479–1491.

Behrenfeld, M.J.; Falkowski, P. (1997b). Photosynthetic rates derived from satellite-based chlorophyll concentration. *Limnology & Oceanography 42(1)*: 1–20.

Campbell, J.; et al., (2002). Comparison of algorithms for estimating ocean primary production from surface chlorophyll, temperature, and irradiance. *Global Biogeochemical Cycles 16(3)* 1035, DOI:10.1029/2002GL015068.

Carr, M.-E., et al. (2006). A comparison of global estimates of marine primary production from ocean color. *Deep-Sea Research II 53*: 741–770.

Carton, J.A.; Chepurin, G.; Cao, X.; Giese, B.S. (2000a). A simple ocean data assimilation analysis of the global upper ocean 1950-1995, part 1: methodology. *J. Physical Oceanography 30*: 294–309.

Carton, J.A.; Chepurin, G.; Cao, X. (2000b). A Simple Ocean Data Assimilation analysis of the global upper ocean 1950-1995 Part 2: results. *J. Physical Oceanography 30*: 311–326.

DuRand, M.D; Olson, R.J. (1996). Contributions of phytoplankton light scattering and cell concentration changes to diel variations in beam attenuation in the equatorial Pacific from flow cytometric measurements of pico-, ultra-, and nanoplankton. *Deep-Sea Research II 43*: 891–906.

Eppley, R.W. (1972). Temperature and phytoplankton growth in the sea. *Fishery Bulletin 70*: 1063–1085.

Garver, S.A.; Siegel, D.A. (1997). Inherent optical property inversion of ocean color spectra and its biogeochemical interpretation: 1. Time series from the Sargasso Sea. *J. Geophysical Research 102*:18607–18625.

Green, R.E; Sosik, H.M. (2004). Analysis of apparent optical properties and ocean color models using measurements of seawater constituents in New England continental shelf surface waters. *J. Geophysical Research 109*: C03026, DOI:10.1029/2003JC001977.

Green, R.E; Sosik, H.M.; Olson, R.J. (2003). Contributions of phytoplankton and other particles to inherent optical properties in New England continental shelf waters. *Limnology & Oceanography 48*: 2377–2391.

Howard, K.L.; Yoder, J.A. (1997). Contribution of the subtropical oceans to global primary production. *In*: Liu, C.-T (Ed.) Proceedings of COSPAR Colloquium on Space Remote Sensing of Subtropical Oceans, Taiwan, pp. 157–168. Pergamon.

Lee Z.P.; Carder K.L.; Arnone, R. (2002). Deriving inherent optical properties from water color: multi-band quasi-analytical algorithm for optically deep waters. *Applied Optics 41*: 5755–5772.

Loisel, H.; Bosc, E.; Stramski, D.; Oubelkheir, K.; Deschamps, P-Y. (2001). Seasonal variability of the backscattering coefficient in the Mediterranean Sea on Satellite SeaWIFS imagery. *Geophysical Research Letters 28*: 4203–4206.

Longhurst, A.; Sathyendranath, S.; Platt, T.; Caverhill, C. (1995). An estimate of global primary production in the ocean from satellite radiometer data. *J. Plankton Research 17*: 1245–1271.

Maritorena, S.D.; Siegel, D.A.; Peterson, A. (2002). Optimization of a semi-analytical ocean color model for global scale applications. *Applied Optics 41*: 2705–2714.

Morel, A. (1991). Light and marine photosynthesis: A spectral model with geochemical and climatological implications. *Progress in Oceanography 26*: 263–306.

Morel, A.; Berthon, J.F. (1989). Surface pigments, algal biomass profiles, and potential productivity of the euphotic layer: relationships reinvestigated in view of remote sensing applications. *Limnology & Oceanography 34(8)*: 1545–1562.

Ondrusek, M.E.; Bidigare, R.R.; Waters, K.; Karl, D.M. (2001). A predictive model for estimating rates of primary production in the subtropical north Pacific Ocean. *Deep-Sea Research II 48(8–9)*: 1837–1863.

Pinkerton, M.H.; Moore, G.F.; Lavender, S.J.; Gall, M.P.; Oubelkheir, K.; Richardson, K.M.; Boyd, P.W.; Aiken, J. (2006). A method for estimating inherent optical properties of New Zealand continental shelf waters from satellite ocean colour measurements. *New Zealand Journal of Marine and Freshwater Research 40*: 227–247.

Platt, T. (1986). Primary production of the ocean water column as a function of surface light intensity: algorithms for remote sensing. *Deep Sea Research Part A. Oceanographic Research Papers 33(2)*: 149–163.

Platt, T.; Sathyendranath, S. (1993). Estimators of primary production for interpretation of remotely sensed data on ocean color. *J. Geophysical Research* 98: 14561–14567.

Siegel, D.A.; Maritorena, S.; Nelson, B. (2005). Independence and interdependencies among global ocean color properties: Reassessing the bio-optical assumption. *J. Geophysical Research*: *C07011*. DOI:10.1029/2004FC002527.

Siegel, D.A.; Maritorena, S.; Nelson, N.B.; Hansell, D.A.; Lorenzi-Kayser, M. (2002). Global distribution and dynamics of colored dissolved and detrital organic materials, *J. Geophysical Research 107(C12), 3228.* DOI:10.1029/2001JC000965.

Stramski, D; Reynolds, R.A.; Kahru, M.; Mitchell, B.G. (1999). Estimation of particulate organic carbon in the ocean from satellite remote sensing. *Science 285*: 239–242.

Westberry, T.; Behrenfeld, M.J.; Siegel, D.A.; Boss, E. (2008) Carbon-based primary productivity modeling with vertically resolved photoacclimation. *Global Biogeochemical Cycles 22,* GB2024. DOI:10.1029/2007gb003078.

APPENDIX 5: DEVELOPMENT OF BIOGEOCHEMICAL DATA LAYER

Prepared by Mark Hadfield.

Data layers

The following layers were developed from annual-average fields from the World Ocean Atlas 2005 Climatology and interpolated to the bottom:

- apparent oxygen utilisation
- oxygen saturation
- oxygen concentration
- phosphate
- nitrate
- silicate
- salinity
- temperature.

The bathymetry dataset (known as “eezbathy”) is a 1-km gridded dataset generated by Ude Shankar from the EEZ tidal model grid. The new temperature and salinity layers should match the original MEC layers reasonably closely, except that they are based on a newer version of the WOA climatology. The "eezbathy" dataset has less spatial detail than other NZ-region gridded bathymetry datasets, but it does not have the common problem of negative depths on some of the sub-antarctic rises. The graphs of the data layers are shown in Figures 5.1–5.8 [note these are scans of the originals].

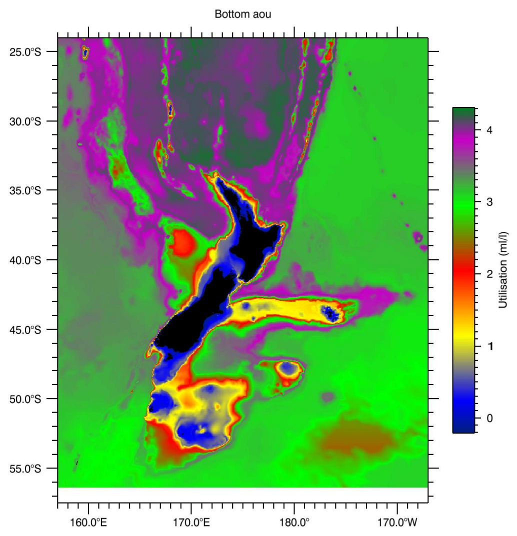

Figure 5.1: Apparent oxygen utilisation.

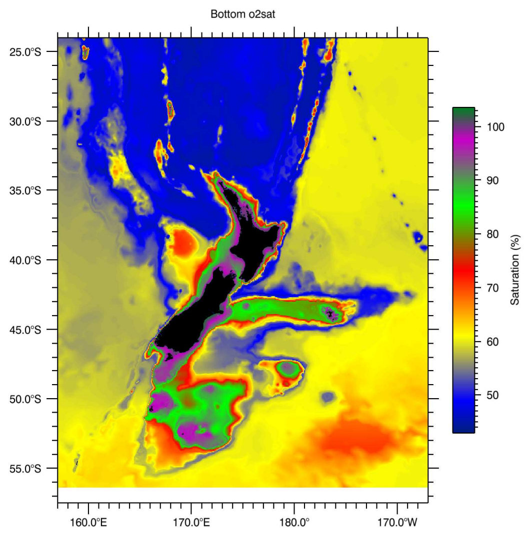

Figure 5.2: Oxygen saturation.

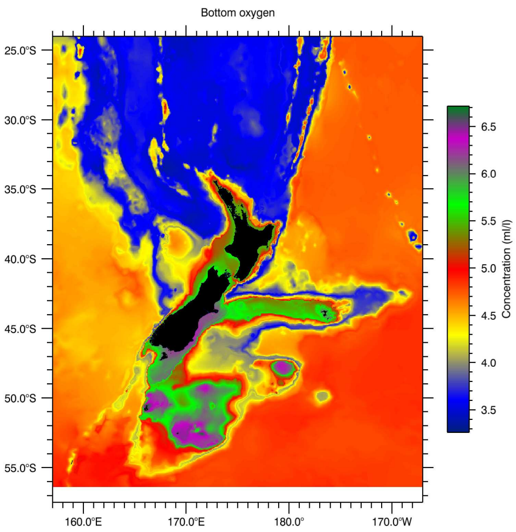

Figure 5.3: Oxygen.

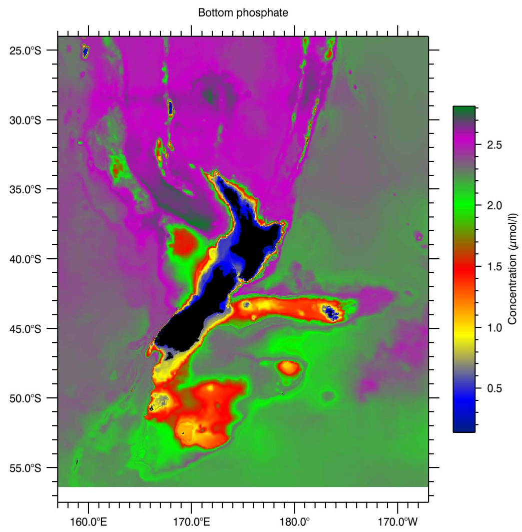

Figure 5.4: Phosphate.

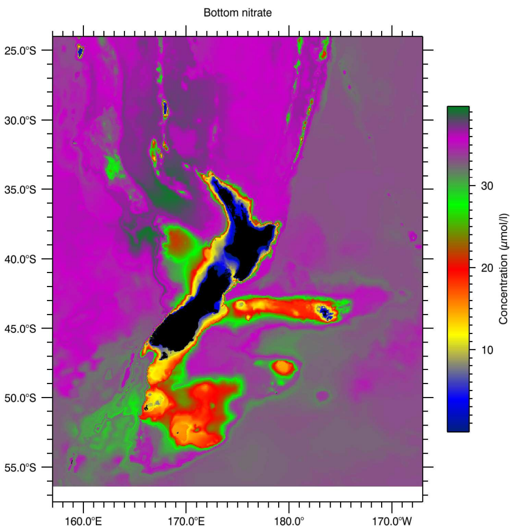

Figure 5.5: Nitrate.

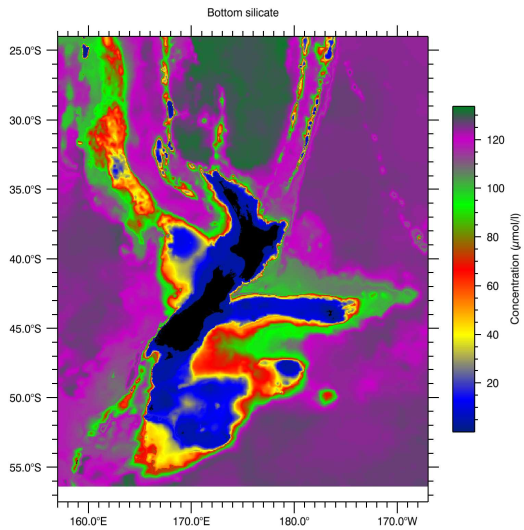

Figure 5.6: Silicate.

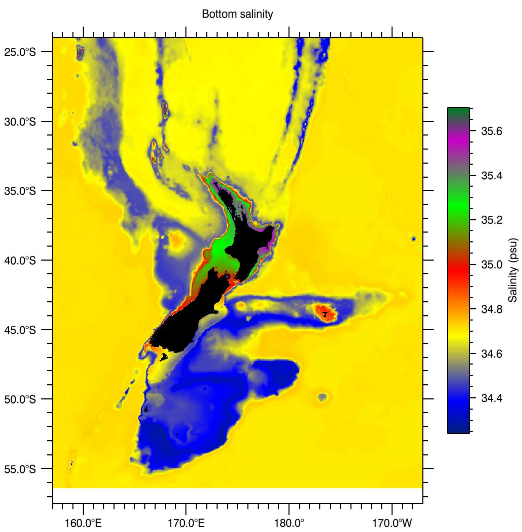

Figure 5.7: Salinity.

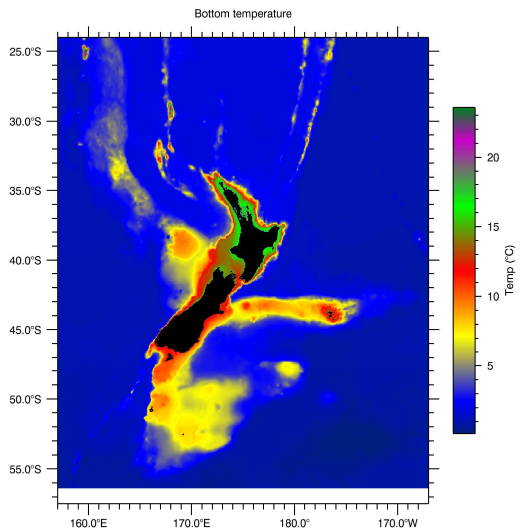

Figure 5.8: Temperature.

APPENDIX 6: GDM FITTED FUNCTIONS

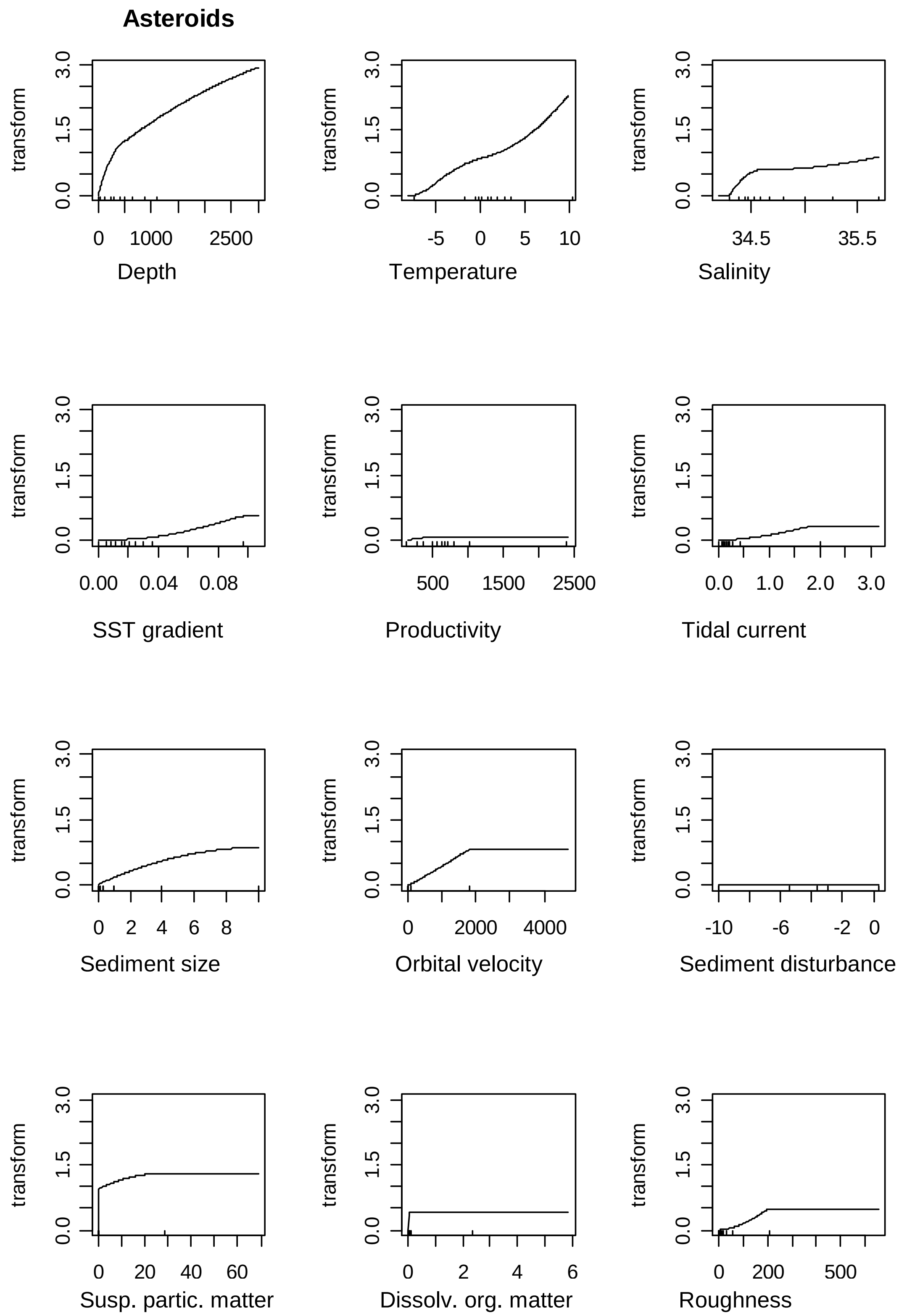

Figure 6.1: Functions fitted by GDM analyses of the relationship between species turnover and environment for the asteroid dataset, averaged across 100 models.

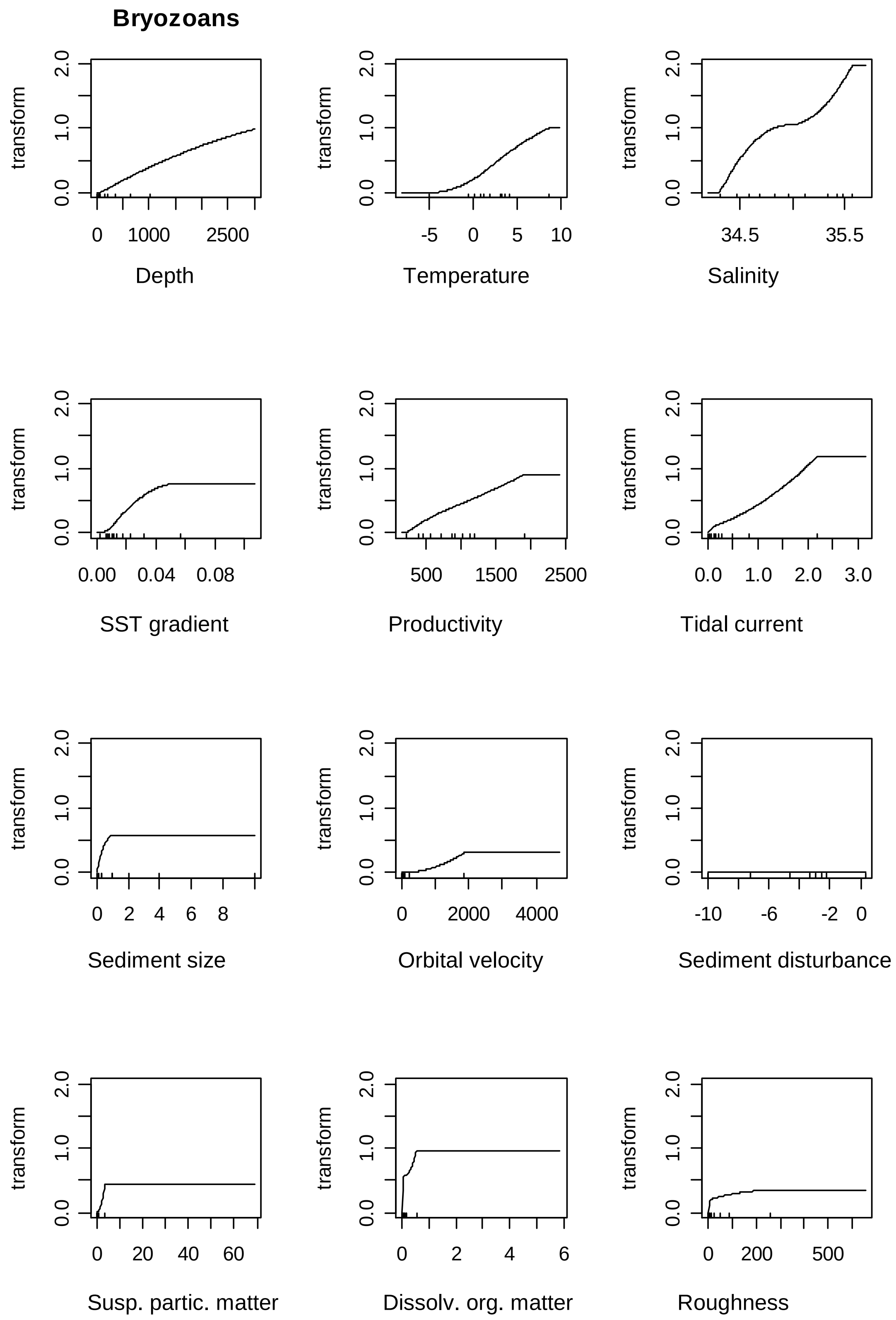

Figure 6.2: Functions fitted by GDM analyses of the relationship between species turnover and environment for the bryozoan dataset, averaged across 100 models.

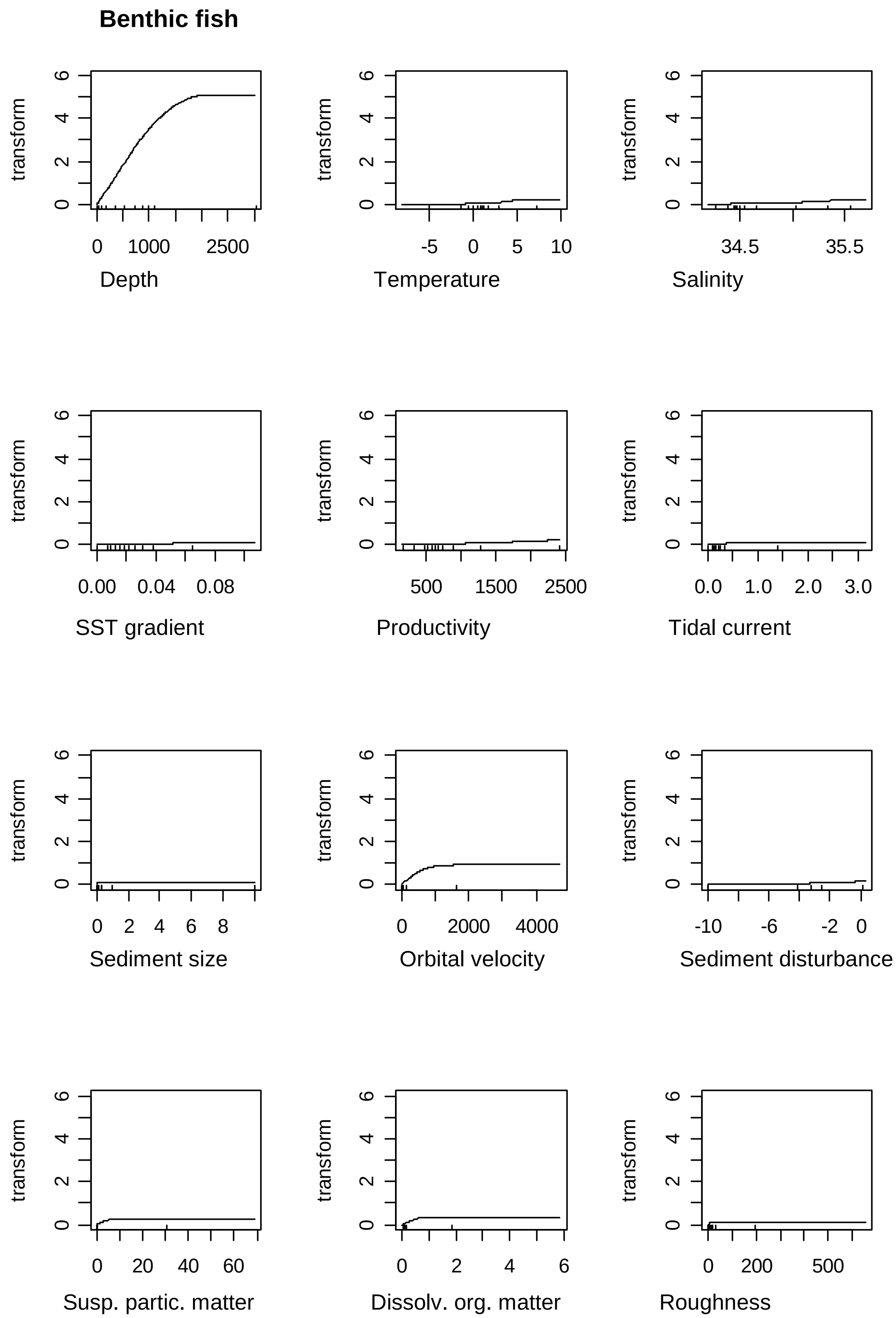

Figure 6.3: Functions fitted by GDM analyses of the relationship between species turnover and environment for the benthic fish dataset, averaged across 100 models.

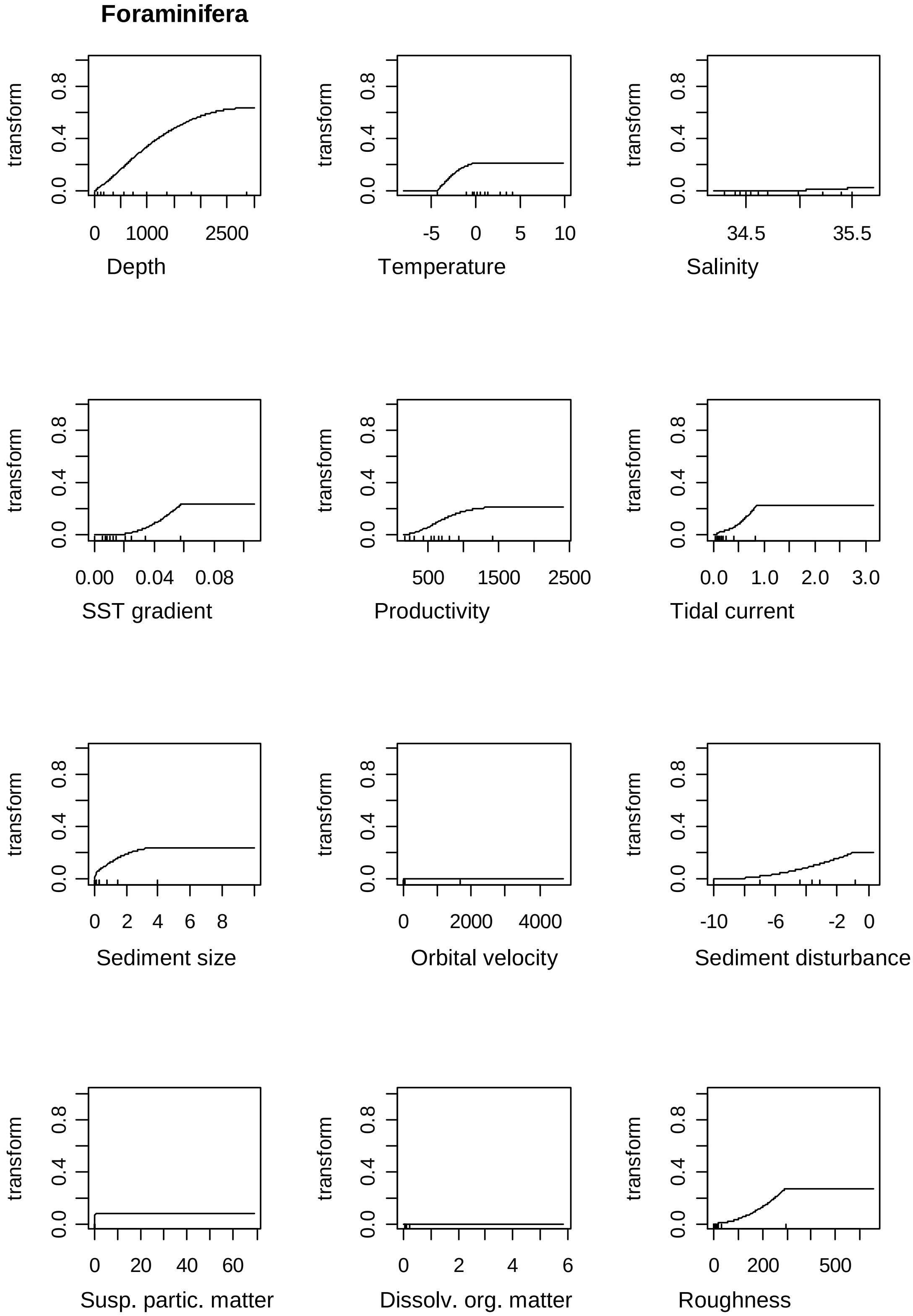

Figure 6.4: Functions fitted by GDM analyses of the relationship between species turnover and environment for the foraminiferan dataset, averaged across 100 models.

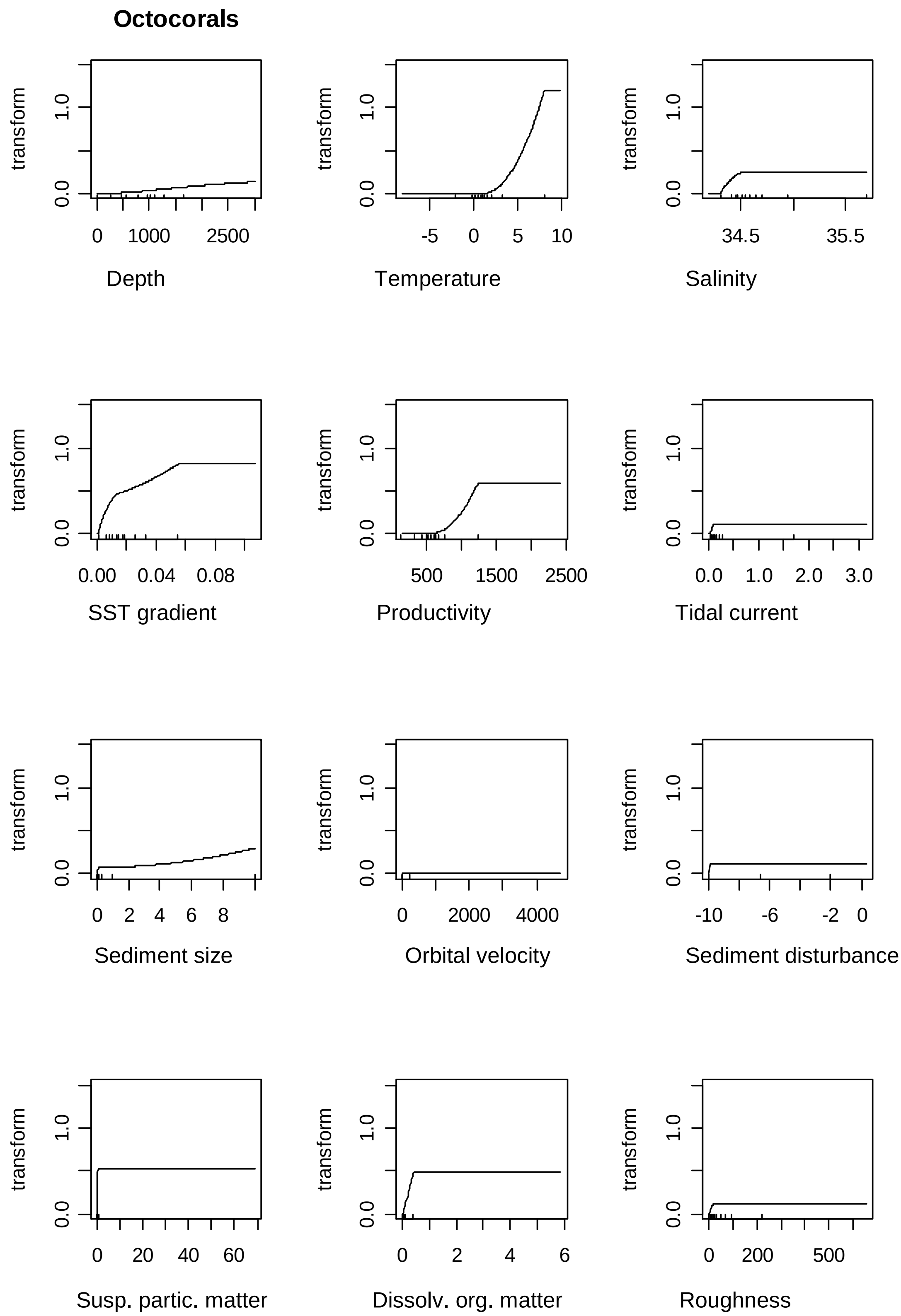

Figure 6.5: Functions fitted by GDM analyses of the relationship between species turnover and environment for the octocoral dataset, averaged across 100 models.

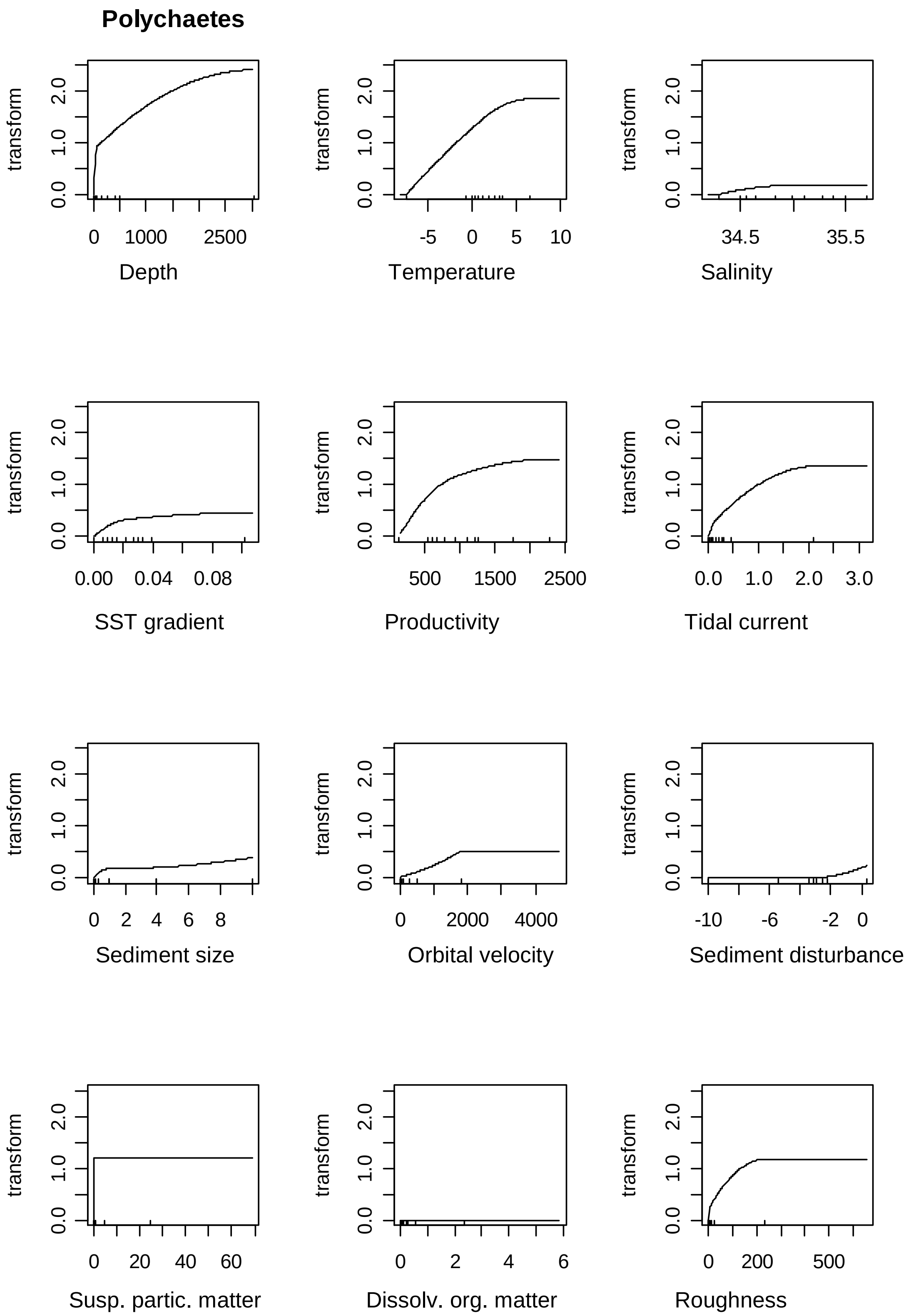

Figure 6.6: Functions fitted by GDM analyses of the relationship between species turnover and environment for the polychaete dataset, averaged across 100 models.

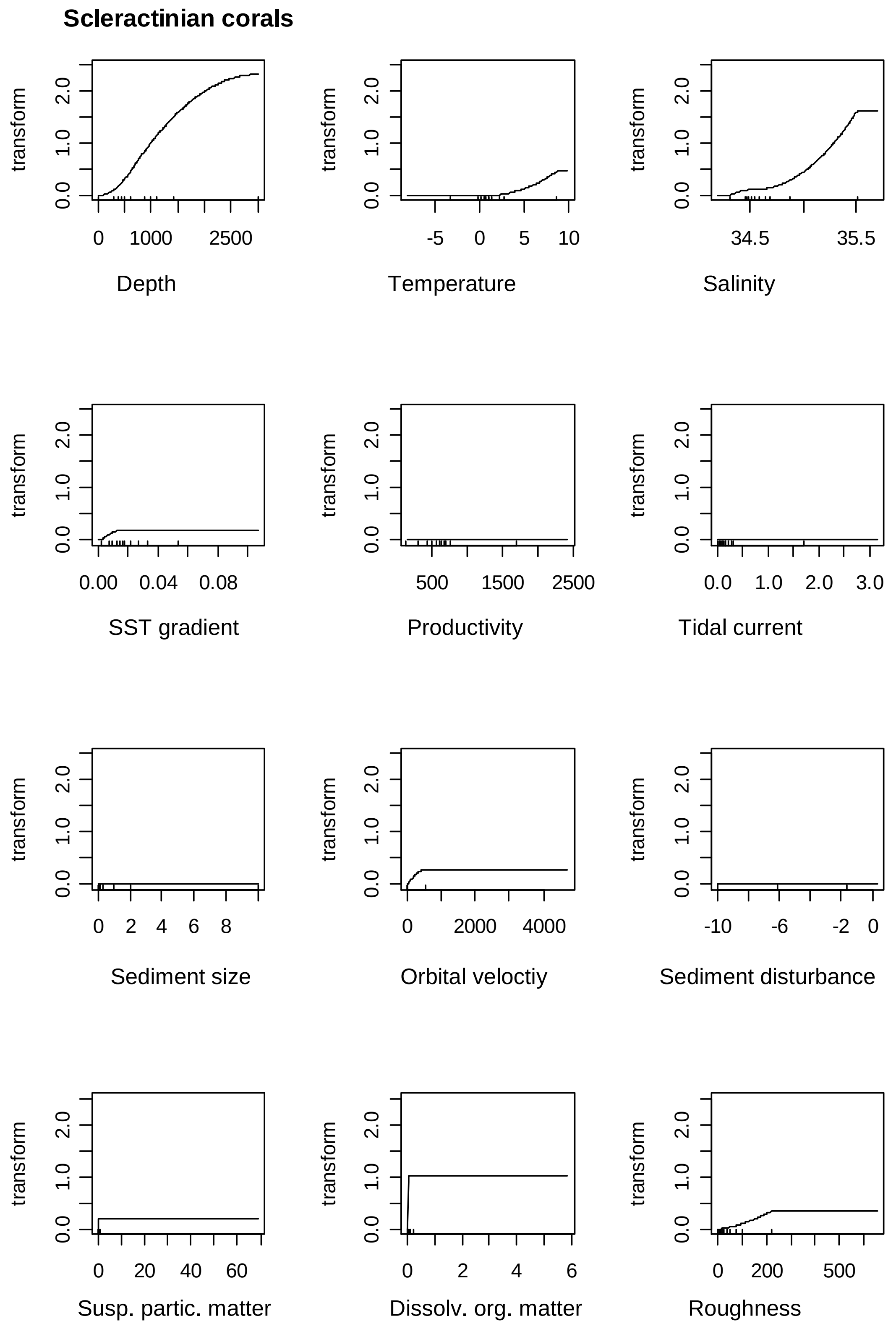

Figure 6.7: Functions fitted by GDM analyses of the relationship between species turnover and environment for the matrix-forming scleractinian coral dataset, averaged across 100 models.

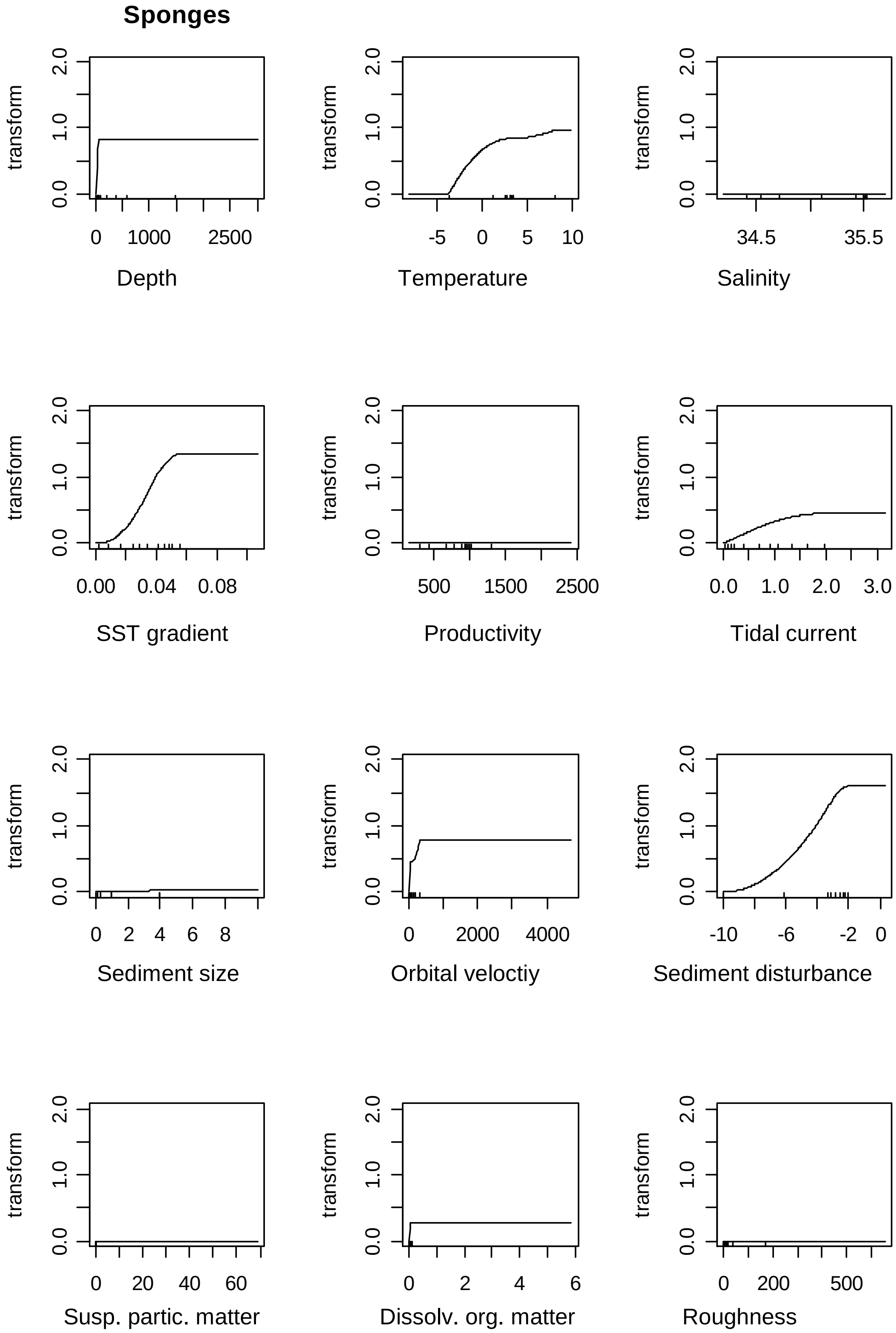

Figure 6.8: Functions fitted by GDM analyses of the relationship between species turnover and environment for the sponge dataset, averaged across 100 models.